Identification of Small-Molecule Enhancers of Arginine Methylation Catalyzed by Coactivator-Associated Arginine Methyltransferase 1

ARTICLE *in* JOURNAL OF MEDICINAL CHEMISTRY · OCTOBER 2012

Impact Factor: 5.45 · DOI: 10.1021/jm301097p · Source: PubMed

16 AUTHORS, INCLUDING:

Fabrizio Dal Piaz
Università degli Studi di Salerno
119 PUBLICATIONS **1,747** CITATIONS
SEE PROFILE

Donghang Cheng
University of Texas MD Anderson Cancer Center
23 PUBLICATIONS **1,225** CITATIONS
SEE PROFILE

Alessandra Tosco
Università degli Studi di Salerno
42 PUBLICATIONS **561** CITATIONS
SEE PROFILE

Gianluca Sbardella
Università degli Studi di Salerno
138 PUBLICATIONS **1,889** CITATIONS
SEE PROFILE

Journal of Medicinal Chemistry

Article

pubs.acs.org/jmc

Identification of Small-Molecule Enhancers of Arginine Methylation Catalyzed by Coactivator-Associated Arginine Methyltransferase 1

Sabrina Castellano,[†] Astrid Spannhoff,[‡] Ciro Milite,[†] Fabrizio Dal Piaz,[†] Donghang Cheng,[‡] Alessandra Tosco,[†] Monica Viviano,[†] Abdellah Yamani,[†,#] Agostino Cianciulli,[†] Marina Sala,[†] Vincent Cura,[⊥] Jean Cavarelli,[⊥] Ettore Novellino,[§] Antonello Mai,[∥] Mark T. Bedford,[‡] and Gianluca Sbardella*[,†]

[†]Dipartimento di Scienze Farmaceutiche e Biomediche, Epigenetic Med Chem Lab, Università degli Studi di Salerno, Via Ponte Don Melillo, I-84084 Fisciano (SA), Italy

[‡]University of Texas M.D. Anderson Cancer Center, Science Park-Research Division, Smithville, Texas 78957, United States

[§]Dipartimento di Chimica Farmaceutica e Tossicologica, Università di Napoli "Federico II", Via D. Montesano 49, I-80131 Napoli, Italy

[∥]Istituto Pasteur—Fondazione Cenci Bolognetti, Dipartimento di Chimica e Tecnologie del Farmaco, Sapienza Università di Roma, P.le A. Moro 5, I-00185 Roma, Italy

[⊥]Département de Biologie Structurale Intégrative, IGBMC (Institut de Génétique et Biologie Moléculaire et Cellulaire), UDS, CNRS, INSERM, 67404 Illkirch Cedex, France

Supporting Information

ABSTRACT: Arginine methylation is a common post-translational modification that is crucial in modulating gene expression at multiple critical levels. The arginine methyltransferases (PRMTs) are envisaged as promising druggable targets, but their role in physiological and pathological pathways is far from being clear due to the limited number of modulators reported to date. In this effort, enzyme activators can be invaluable tools useful as gain-of-function reagents to interrogate the biological roles in cells and in vivo of PRMTs. Yet the identification of such molecules is rarely pursued. Herein we describe a series of aryl ureido acetamido indole carboxylates (dubbed "uracandolates"), able to increase the methylation of histone (H3) or nonhistone (polyadenylate-binding protein 1, PABP1) substrates induced by coactivator-associated arginine methyltransferase 1 (CARM1), both in in vitro and cellular settings. To the best of our knowledge, this is the first report of compounds acting as CARM1 activators.

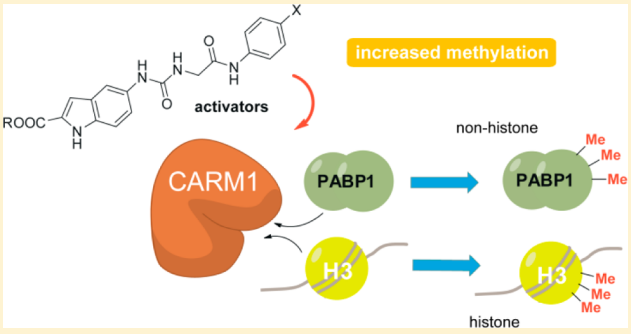

INTRODUCTION

The methylation of arginine residues is a prevalent post-translational modification found on both nuclear and cytoplasmic proteins, which is involved in a number of different cellular processes, including transcriptional regulation, RNA metabolism, and DNA damage repair.[1−4] Enzymes of the protein arginine *N*-methyltransferase (PRMT) family catalyze the transfer of a methyl group from the donor *S*-adenosyl-L-methionine (SAM or AdoMet) to the guanidinium side chain of arginine residues in the target protein, resulting in methylated arginine and *S*-adenosyl-L-homocysteine (SAH or AdoHcy).[5−7] This post-translational modification mainly occurs on glycine-and arginine-rich patches (GAR motifs) within their substrates,[8] and its complexity is enhanced by the ability of the arginine residue to be methylated in three different ways on the guanidino group: ω-N^G-monomethylated (MMA), symmetrically ω-N^G, ω-N'^G-dimethylated (sDMA), and asymmetrically ω-N^G, N^G-dimethylated (aDMA), each of which has potentially different functional consequences.[2,7,9] To date, nine proteins, differing in sequence and in length, have been clearly identified as PRMTs in mammals and are classified as type I, type II, or type III enzymes.[5,7,9] These enzyme types all methylate the terminal (or ω) guanidino nitrogen atoms, but type I PRMTs (PRMT1−4, PRMT6, and PRMT8) catalyze the production of aDMA, whereas type II PRMTs (PRMT5/JBP1, PRMT7) catalyze the formation of sDMA. PRMT7 has been described as also having type III activity on certain substrates.[10] In addition, a type IV enzyme that catalyzes the monomethylation of the internal (or δ) guanidino nitrogen atom has been described in yeast.[7,9]

Received: July 26, 2012
Published: October 24, 2012

Chart 1. Selected Small-Molecule Inhibitors of PRMTs

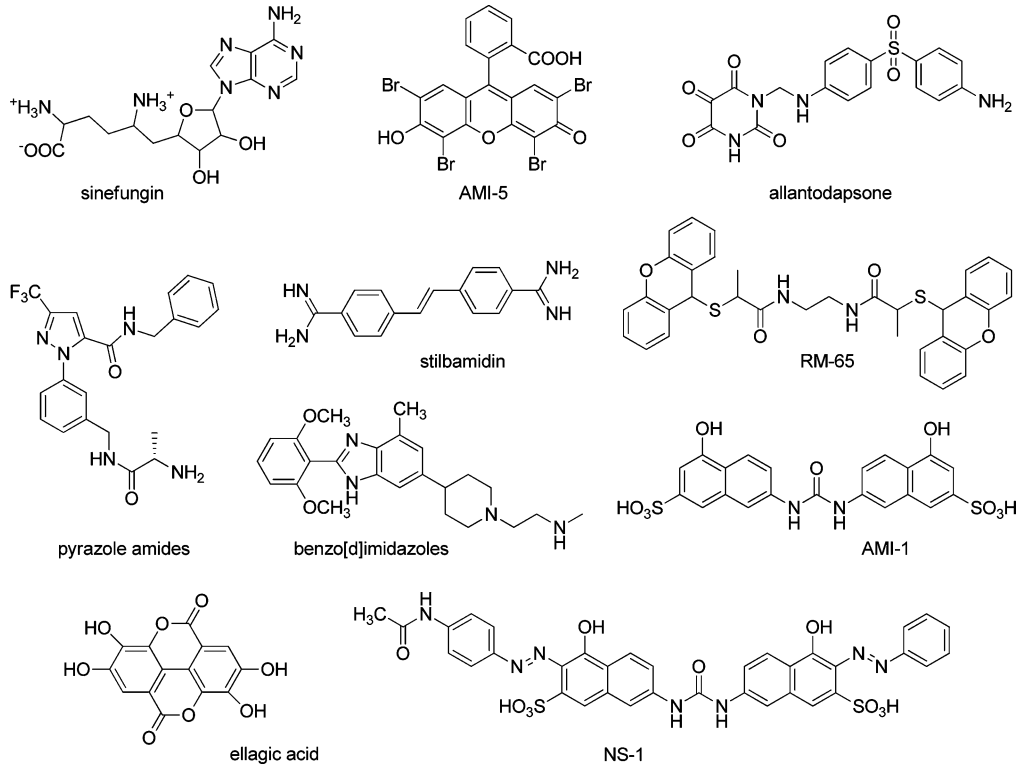

A growing number of studies have recently recognized the nearly ubiquitous expression of PRMTs (with the exception of PRMT8, which is a neuron-specific enzyme[11,12]) in most mammalian cell types and tissues, as well as their involvement in a wide variety of functional processes like RNA processing, DNA damage and repair, cell signaling, and most importantly in transcription.[9,13] Moreover, arginine methylation of histones can increase the complexity of the histone code by modulating the interaction of nuclear factors with other nearby histone marks.[14−16]

In mammalian cells, bulk protein arginine methylation is likely ascribable to PRMT1, the main PRMT member. This enzyme is involved in the dysregulation of nuclear receptor signaling,[2,5,17,18] which is a hallmark of hormone dependent cancers, e.g., breast cancer.[19−22] Recently, it was shown that PRMT1 is a component of mixed lineage leukemia (MLL) transcription complex and that its activity is required for malignant transformation.[23] Moreover, several tumors, including breast cancer[24,25] and colon cancer,[26,27] are characterized by aberrant expression of spliced forms of PRMT1, while deregulation of the histone H4R3 methyl mark (a major cellular substrate of PRMT1[18]) is a predictor of prostate cancer.[28]

Similarly, PRMT4 (commonly referred to as coactivator-associated arginine methyltransferase 1 (CARM1)) plays a crucial role in modulating gene expression at multiple critical levels,[5] methylating many coactivators, including p300/CBP and amplified in breast cancer-1 (AIB1),[2] as well as proteins involved in splicing[29] and RNA-binding proteins.[30−32] CARM1 has been implicated in spinal muscular atrophy pathogenesis[29] and has been associated with viral infections involving human T lymphotrophic virus.[33] Recently, it has been reported that CARM1 is overexpressed in both aggressive prostate cancer and breast tumor[34,35] and that the presence of CARM1 and the increased H3R17 methylation give an important contribution in breast cancer (particularly estrogen receptor α dependent) manifestation and progression.[36,37] Furthermore, CARM1 and PRMT1, together with p300/CBP and PARP1, synergistically coactivate NF-κB-dependent gene expression[38] and cooperate in p53-dependent transcriptional activation.[39] In addition to this, PRMTs have also emerged as potential new targets for the development of a novel therapeutic for heart disease,[34,35,40−45] as they are overexpressed in the hearts of patients with coronary heart disease[46] and PRMT activity appears to be responsible for generating the majority of the aDMA, which subsequently blocks NO production and causes many cardiovascular conditions such as diabetes and hypertension.[47−49]

On the other hand, PRMT1 and CARM1, together with PRMT5, are downregulated in senescent tissues,[50] and it has been reported that the activity of CARM1 is required for the proper mainteinance of physiological processes like endochondral ossification and chondrocyte proliferation,[51] myogenesis,[52] glycogen metabolism,[53] and proper control of proliferation and differentiation of pulmonary epithelial cells.[54]

Therefore, there is convincing evidence that PRMTs have a crucial role in several serious human diseases as well as in many important physiological processes,[55,56] supporting the hypothesis that targeting PRMTs would be a viable approach for drug discovery efforts.[57−60]

As a matter of fact, extensive research has been conducted to better understand the role of PRMTs in physiological and pathological pathways,[5,17−22,34,35,40−43,45,54,61−63] to elucidate the structure[64−69] of these enzymes, and to gain insights into the mechanism of methyl transfer.[70,71] Yet, the number of small molecule modulators of the PRMTs reported to date is still limited (Chart 1).[13,60,67,72−99]

dx.doi.org/10.1021/jm301097p | J. Med. Chem. 2012, 55, 9875−9890

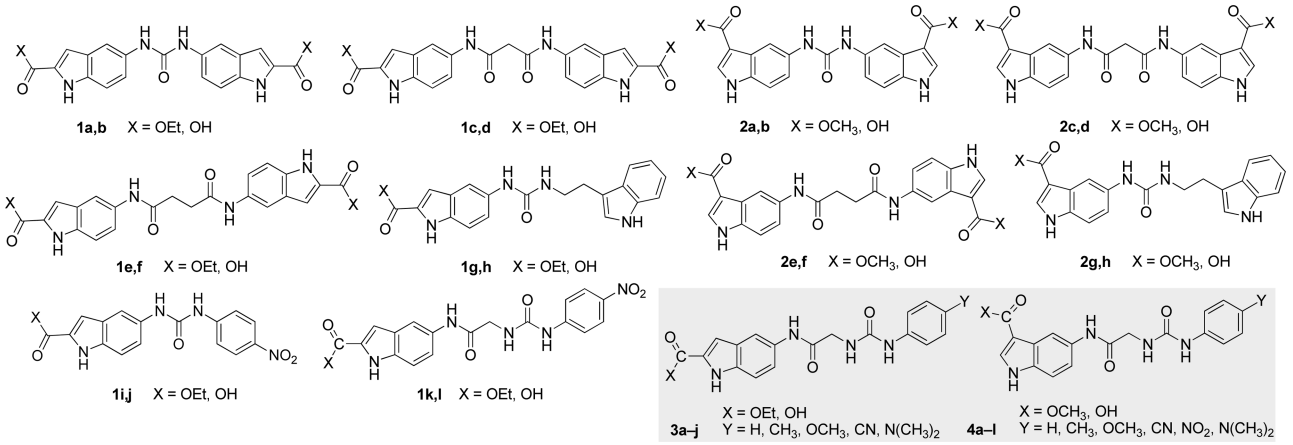

Figure 1. Indole derivatives **1a–l**, **2a–h**, **3a–j**, and **4a–l**.

Scheme 1. Synthesis of Derivatives 1k,l, 3a–j and 4a–l[a]

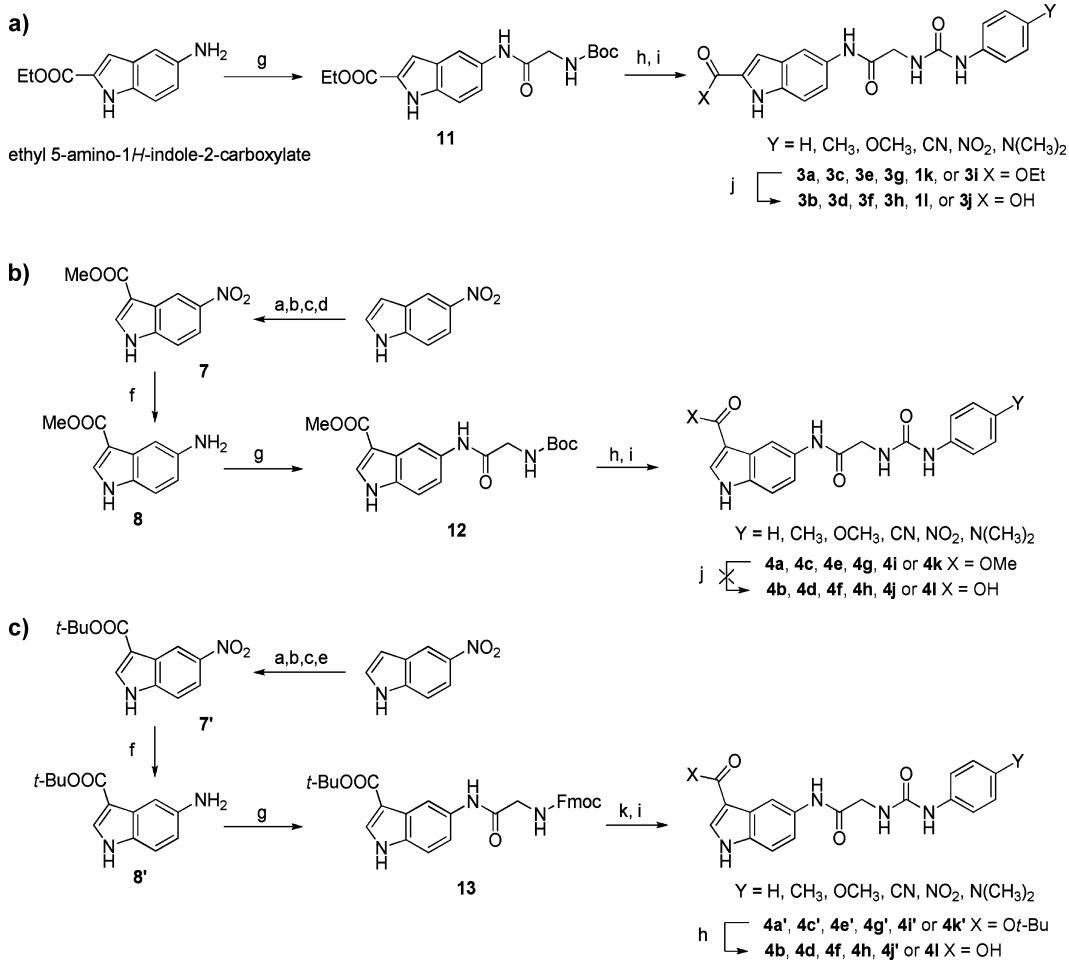

[a]Reagents and conditions: (a) $(COCl)_2$, Et_2O, 0 °C, overnight; (b) KOH, H_2O, reflux, 2 h; (c) H_2O_2 (10% wt in H_2O), reflux, 4 h; (d) H_2SO_4, MeOH, reflux, 6 h; (e) *t*-BuOH, DCC, TEA, DMF, 120 °C, 3h; (f) H_2 (1 atm), 5% Pd/C, EtOH, 2 h; (g) Boc-Gly-OH or Fmoc-Gly-OH, DIEA, HOBt, HBTU, THF/DMF 7:2, rt, overnight; (h) TFA/CH_2Cl_2 1:3, rt, 30 min; (i) isocyanate, TEA, THF, rt, 3 h; (j) NaOH, pyridine, H_2O/THF 4:1, rt, overnight; (k) CH_2Cl_2/piperidine, rt, 30 min.

In 2004, a small-molecule screening study led some of us to the identification of the symmetric urea derivative arginine methyltransferase inhibitor 1 (AMI-1, Chart 1) as a selective arginine methylation specific inhibitor, noncompetitive with *S*-adenosylmethionine (SAM) binding and not affecting lysine methylation.[75] By molecular modeling studies, we then proposed that AMI-1 spans both the SAM and Arg binding sites without fully occupying them.[78] This binding hypothesis, consistent with the fact that AMI-1 does not inhibit UV cross-linking of SAM to PRMT1 (suggesting that it does not

dx.doi.org/10.1021/jm301097p | J. Med. Chem. 2012, 55, 9875–9890

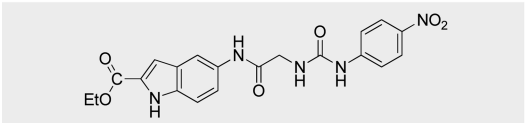

	% inhibition (at 50 μM, mean ± SD)				
	PRMT1 (H4)	PRMT3 (GAR)	CARM1 (H3)	PRMT6 (H3)	SET7 (H3)
1k	27.7 ± 0.5	54.7 ± 1.7	-175.5 ± 2.6	-19.3 ± 0.3	10.2 ± 0.2
AMI-1	87.7 ± 1.7	101.2 ± 2.9	74.8 ± 1.9	40.7 ± 1.1	34.3 ± 0.7

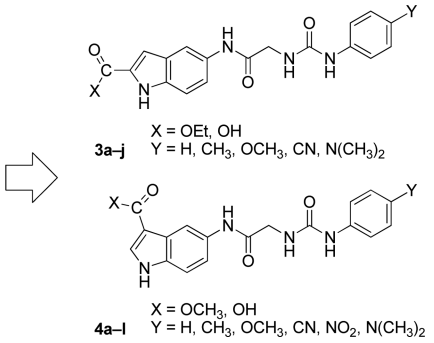

Figure 2. CARM1/PRMT4 activators **3a–j** and **4a–f**.

compete for the SAM binding site),[75] was subsequently supported by structure-based 3-D QSAR models[100] and allowed us to design and synthesize carboxy analogues of AMI-1 that are nearly as potent as the parent compound while retaining PRMT selectivity.[92]

Pursuing our efforts toward the identification of potent and selective PRMT inhibitors, we replaced the hydroxynaphthalene moiety with the bioisosteric indole framework, a "privileged" structural motif commonly found in pharmaceutical drugs and natural products.[101] Thus, we prepared 2,5-disubstituted indole derivatives **1a–l** as well as their positional isomers **2a–h** (Figure 1), and, in conformity with our previous studies,[78,92] we performed a preliminary screening of their activities against human recombinant PRMT1 and other methyltransferases in vitro. Surprisingly, we found that the ureidoacetamido-indole derivative **1k**, though scarcely active in inhibiting PRMT1 (and other methyltransferases, see below), induced a marked activation of CARM1/PRMT4. Therefore, in this paper, we describe the synthesis of a series of ureidoacetamido-indole derivatives **3a–j** and **4a–l** (Figure 1), structurally related to **1k**, and the evaluation of the effects on CARM1-induced arginine methylation.

CHEMISTRY

The synthesis of 2,5-disubstituted indole derivatives **1a–j** as well as of 3,5-substituted analogues **2a–h** is reported in Supporting Information (Schemes S1 and S2, respectively).

Derivatives **1k,l** and **3a–j** were prepared (Scheme 1A) starting from 5-amino-1*H*-indole-2-carboxylate, which was in turn prepared through Fisher indole reaction and subsequent reduction using hydrogen over palladium on activated carbon, as previously described.[102,103]

The reaction of 5-amino-1*H*-indole-2-carboxylate with *N*-(*tert*-butoxycarbonyl)glycine (Boc-Gly-OH) in the presence of the peptide coupling reagents hydroxybenzotriazole (HOBt) and *O*-benzotriazole-*N*,*N*,*N*′,*N*′-tetramethyl-uronium-hexafluoro-phosphate (HBTU) and Hünig's base (*N*,*N*-diisopropylethylamine, DIEA) to obtain the Boc-protected glycinamide **11**, which was deprotected with trifluoroacetic acid and then coupled with the proper phenylisocyanate in the presence of triethylamine to yield the esters **1k**, **3a**, **3c**, **3e**, **3g**, and **3i**. The hydrolysis of the latter finally gave the corresponding acids **1l**, **3b**, **3d**, **3f**, **3h**, and **3j**, respectively.

A similar synthetic procedure (Scheme 1B) yielded the esters **4a**, **4c**, **4e**, **4g**, **4i**, and **4h** starting from 5-amino-1*H*-indole-3-carboxylate **8**,[104] obtained by catalytic hydrogen reduction of the corresponding 5-nitro derivative **7**, prepared by reaction of 5-nitroindole with oxalyl chloride and subsequent alkaline hydrolysis, oxidative decarboxylation and, finally, esterification, according to a slight modification of a previously described procedure.[105] Curiously, any attempt to hydrolyze the aforementioned esters failed to give the acids **4b**, **4d**, **4f**, **4h**, **4j**, and **4l**, which were, instead, obtained from the corresponding *tert*-butyl esters **4a′**, **4c′**, **4e′**, **4g′**, **4i′**, and **4h′** (prepared starting from *tert*-butyl 5-amino-1*H*-indole-3-carboxylate **8′**) after treatment with trifluoroacetic acid in dichloromethane (Scheme 1C).

RESULTS AND DISCUSSION

Identification of CARM1 Activators. In pursuing our campaign aimed at the identification of potent and selective PRMT inhibitors, we synthesized derivatives **1a–l** and **2a–h** and tested them against human recombinant PRMT1 (hPRMT1) in vitro, using as a substrate the RNA-binding nuclear shuttling protein Npl3, specifically methylated by both yeast (HMT1)[106–108] and human (PRMT1) orthologues,[75] determining the percent values of inhibition at the fixed doses of 10 and 50 μM (Tables S1 and S2, respectively, Supporting Information). AMI-1[75] and EML108[92] were used as reference compounds.

Even though none of the derivatives **1a–l** were efficient inhibitors of PRMT1 (Supporting Information Table S1), compounds that displayed a greater than 60% inhibition were retested at 50 μM against recombinant PRMT1, PRMT3, CARM1, and PRMT6, using histone H4, the glycine- and arginine-rich (GAR) motif, and histone H3 (for both CARM1 and PRMT6) as substrates, respectively (not shown). We noticed that, albeit scarcely active in inhibiting the other enzymes, ureidoacetamido-indole derivative **1k** induced a marked activation of CARM1/PRMT4 (Figure 2). We repeated the assay by testing the compound at six different concentrations (3, 6, 12, 25, 50, and 100 μM) against CARM1 using as a substrate the polyadenylate-binding protein 1 (PABP1), an in vivo major substrate for CARM1.[31] Again, compound **1k** induced a marked and dose-dependent increase in the enzyme activity, clearly noticeable even at the lowest tested concentration (3 μM, Figure 3). A similar result was observed when H3 was used as a substrate (Figure S1, Supporting Information). Therefore, we prepared the analogues **3a–j** and the corresponding positional isomers **4a–l** (Figure 2) and test all of them (with the exception of the acids of the series **4**)[109] at 50 μM in an in vitro assay, to assess their potency against CARM1, using H3 and PABP1 as substrates.

As reported in Table 1 (and also in the fluorographs in Figure S2, Supporting Information), all compounds **3** (with the only exception of dimethylamino-substituted carboxylic acid **3j**) induced, even if with different potency, an increase in H3 methylation catalyzed by CARM1, further substantiating the

dx.doi.org/10.1021/jm301097p | J. Med. Chem. 2012, 55, 9875–9890

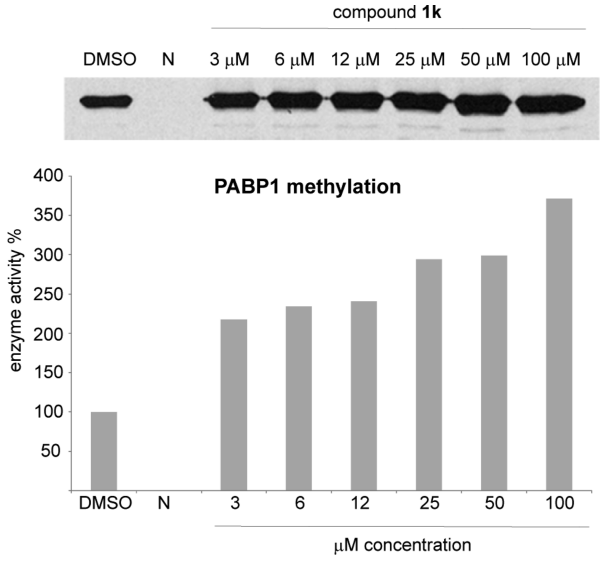

Figure 3. Activation of enzymatic activity of CARM1 after treatment with **1k** (3, 6, 12, 25, 50, and 100 μM) using PABP1 as a substrate. The bands were cut out and the efficiency of the enzyme was determined by scintillation counting. DMSO was used as positive control. N stands for negative control (no SAM added).

relationship between such effect and the lead scaffold of this series of molecules. The substituents decorating the benzene moiety seem to modulate the intensity of the enzymatic activation, the highest effect being detected with the introduction of a methoxy group (derivatives **3e** and **3f**), which yielded an increase in CARM1 activity even more significant (183% and 211%, respectively) than what we previously observed for nitro-substituted derivatives **1k** and **1l** (Table 1).

On the other hand, the effects of derivatives **3** on the methylation of the nonhistonic substrate PABP1 were less regular. In fact, the methyl-, the cyano-, and the nitro-substituted esters **3c**, **3g**, and **1k**, respectively, caused a very strong amplification of substrate methylation (382%, 358%, and 299%, respectively), whereas the unsubstituted acid **3b** as well as the methyl- and the dimethylamino-substituted acids **3d** and **3j** determined a lesser effect (172%, 149%, and 135%, respectively).

Regarding compounds **4**, positional isomers of **3**, in general they produced a reduction of methylation of both substrates, more evident in the case of PABP1 (Table 1). The only exceptions are the cyano- and the dimethylamino-substituted esters **4g** and **4k**, which yielded a moderate gain in H3 methylation (135% and 125%, respectively) while inhibiting PABP1 methylation, and the nitro-substituted ester **4i**, which determined a slight augmentation of the methylation on both substrates (134% for H3 and 115% for PABP1). It is noteworthy that derivatives **3a**, **3j**, and **4k** seem to be endowed with a unique activity profile, apparently being capable of amplifying the methylation levels of one substrate while inhibiting the CARM1 induced methylation of the other (Table 1). All tested derivatives were basically inactive against PRMT1/Npl3p even at 50 μM concentration (Table S4, Supporting Information).

SPR-Based Binding Assay. The different effects of ureidoacetamido indole derivatives **3** and **4** on the methylation of histone or nonhistone substrates could be due to various reasons, among which are (a) different enzyme approaching

Table 1. Effects of Compounds 3a–j and 4a–l (50 μM) on CARM1-Catalyzed Methylation of Histone- Or Nonhistone Substrates[a]

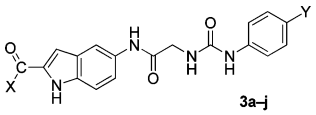

3a–j

X = OEt, OH
Y = H, CH_3, OCH_3, CN, $N(CH_3)_2$

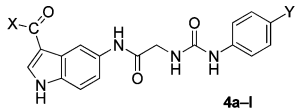

4a–l

X = OCH_3, OH
Y = H, CH_3, OCH_3, CN, NO_2, $N(CH_3)_2$

			% CARM1 activity[b] at 50 μM (mean ± SD[c])	
compd	X	Y	H3[d]	PABP1[e]
3a	OEt	H	134.1 ± 2.8	10.5 ± 0.5
3b	OH	H	167.1 ± 4.0	172.3 ± 5.3
3c	OEt	CH_3	127.2 ± 2.6	382.3 ± 3.1
3d	OH	CH_3	111.0 ± 0.8	148.8 ± 2.5
3e	OEt	OCH_3	182.7 ± 2.0	74.7 ± 0.7
3f	OH	OCH_3	211.2 ± 1.5	96.3 ± 0.4
3g	OEt	CN	115.4 ± 0.7	357.6 ± 3.9
3h	OH	CN	142.7 ± 1.5	81.2 ± 0.7
1k[f]	OMe	NO_2	175.5 ± 2.6	298.9 ± 5.7
1l[f]	OH	NO_2	142.5 ± 1.0	85.3 ± 0.5
3i	OEt	$N(CH_3)_2$	101.7 ± 0.8	70.6 ± 0.8
3j	OH	$N(CH_3)_2$	48.3 ± 0.9	134.7 ± 2.1
4a	OMe	H	74.7 ± 0.7	26.5 ± 0.1
4b	OH	H	ND[g]	ND[g]
4c	OMe	CH_3	39.7 ± 1.1	4.7 ± 0.1
4d	OH	CH_3	ND[g]	ND[g]
4e	OMe	OCH_3	62.7 ± 0.6	28.2 ± 0.4
4f	OH	OCH_3	ND[g]	ND[g]
4g	OMe	CN	134.9 ± 1.5	38.8 ± 0.2
4h	OH	CN	ND[g]	ND[g]
4i	OMe	NO_2	134.2 ± 2.4	114.7 ± 2.0
4j	OH	NO_2	ND[g]	ND[g]
4k	OMe	$N(CH_3)_2$	125.2 ± 0.7	7.6 ± 0.1
4l	OH	$N(CH_3)_2$	ND[g]	ND[g]
EML108			83.1 ± 0.8	NT[h]
AMI-1			74. ± 1.9	NT[h]

[a]Values are means determined for at least two separate experiments. [b]Enzyme activity percentage, calculated with respect to DMSO. [c]Standard deviation values are indicated in percentage points. [d]Histone H3 (1.1 μM) and SAM (0.42 μM) were used as substrates. [e]PABP1 was used as a nonhistone substrate, SAM as cofactor (see Experimental Section). [f]Compounds **1k** and **1l** were inserted for comparison and their activities were obtained from previous experiments. [g]Not detectable (see ref 111.). [h]Not tested.

directions for the two substrates, (b) binding of the small molecule to an allosteric site resulting in a conformational change of the enzyme structure, leading to a better affinity for one substrate and a worse affinity for the other, (c) interaction of the small molecule with the substrates themselves, thus improving or worsening their molecular recognition by the enzyme catalytic site.

As a matter of fact, Zheng and co-workers recently proposed that AMI-1 and structurally related compounds preferentially interact with the histone peptide rather than the enzyme.[87] Similarly, Kundu and co-workers found that ellagic acid (Chart 1), one component of pomegranate extract, specifically inhibits CARM1-induced methylation at arginine 17 of histone H3 (H3R17) by binding to a "KAPRK" motif of the substrate.[90]

Therefore, we resolved to ascertain if the observed activity of the compounds on protein methylation could be due (at least

dx.doi.org/10.1021/jm301097p | J. Med. Chem. 2012, 55, 9875–9890

partially) to a direct interaction with the substrate. To this aim, we took advantage of a surface plasmon resonance-based (SPR-based) binding assay as implemented with Biacore technology, recently set up and successfully employed by us to study in real-time kinetic and thermodynamic parameters of ligand−protein interactions between KAT3B and small-molecule derivatives.[110,111]

In a first set of experiments, calf thymus histone H3 or a peptide from PABP1 comprising residues 437−488 (thus containing the two arginine residues, R455 and R460, that have been reported to be methylated by CARM1)[31] were immobilized (17000 RU, response units)[112] on different flow cells of the biosensor chip and different concentrations (50−10000 nM) of derivatives **1k**, **3c**, **3g**, and **4e** were injected over the peptide surface. Both AMI-1[75] and ellagic acid[90] were used as reference compounds.

To reduce false positives from detergent-sensitive nonspecific aggregation-based binding,[113] 0.005% NP40 was added to the running buffer in all the experiments.[114] To evaluate possible unspecific bindings, all compounds were also injected on an immobilized bovine serum albumin (BSA). The binding of each compound was read out in real time as the change in mass at the sensor surface. After injection, running buffer was flowed over the surface and dissociation of the compounds from the surface was observed (Figure S3, for derivatives 1k and 3g, and Figure S5, for derivatives 3c and 4e, Supporting Information).

Consistently with previous reports,[87,90] both reference compounds, AMI-1 and ellagic acid, interacted efficiently (affinity constant K_D = 671 nM and 172 nM, respectively) with the immobilized histone H3 substrate, as shown by the concentration-dependent responses and the clearly evident exponential curves during both the association and dissociation phases (Figure S4, Supporting Information). Yet, the interaction with PABP1(437−488) was barely perceptible (if any; not shown). SPR experiments carried out on tested compounds also produced good sensorgrams but showed very low and/or concentration-independent responses, thus suggesting negligible interactions of such molecules with either histone (Figure S3, panels A,D, Supporting Information) or nonhistone substrates (Figure S3, panels B,E, Supporting Information).

Next, we turned our attention to the investigation of the binding to CARM1. It has been reported that SAM binding to CARM1 induces the formation of a helix that serves as a binding ridge for the protein substrate.[64,67] Therefore, the presence of the cofactor is crucial for the formation of the enzyme active complex. Yet, commercially available SAM is contaminated by various amounts of *S*-adenosylhomocysteine (SAH) and, moreover, a nonenzymatic pseudo-first-order formation of SAH spontaneously occurs in aqueous medium by the transfer of methyl groups from SAM to water forming methanol.[115,116] On the other hand, the commercially available and inexpensive SAH is quite stable and binds efficiently to the enzyme, thus being an excellent replacement for the cofactor in biophysical studies.[67] Therefore, we immobilized full length GST-tagged CARM1 on the biosensor chip (12000 RU) and validated the immobilization by injecting either histone H3 or PABP1(437−488) at different concentrations (50−4000 nM), in the presence of 200 μM SAH, obtaining K_D values of 6.5 and 158 nM, respectively (Figure S3, panels G and J, Supporting Information). As shown in Figure S3C,F, Supporting Information, no interaction was observed after injection of compounds **1k** and **3g** (in the range 50−10000 nM) on the surface of the immobilized enzyme, both in the presence and in absence (not shown) of SAH. Conversely, the presence of 4 μM **1k** or **3g** affects the affinity of the substrate for the complex enzyme/SAH (panels H,K and I,L). Similar results were obtained with compounds **3c** and **4e** (Figure S5, Supporting Information). It is noteworthy that, under the same conditions AMI-1 binds to the protein with a K_D value of 810 nM (Figure S4, Supporting Information). Together with the aforementioned results from the analysis of the interaction with the substrates, this outcome suggests that the inhibition of CARM1 activity showed by AMI-1[75] may be not completely due to an interaction with the substrate as recently proposed,[87] at least when PABP1 is used as a substrate. To evaluate possible unspecific bindings, all compounds were also injected on an immobilized bovine serum albumin (BSA), and no interaction was observed (data not shown).

Cellular Activity of CARM1 Activators. Then, we resolved to determine whether the increase of CARM1 induced arginine methylation after treatment with compounds **3** was maintained within a cellular context. The cell-based reporter system we previously developed for PRMT1 activity[75,92] was inadequate to this purpose, as CARM1 does not methylate Npl3p. On the contrary, PABP1 is a major CARM1 substrate[31] and in CARM1 knockout cells it is hypomethylated.[117] Moreover, CARM1 is the only enzyme that methylates PABP1. An accurate gauge of CARM1 activity should be performed starting from unmethylated PABP1, yet the methyl mark is extremely stable, as no arginine demethylases have been hitherto discovered,[9] thus a cell-based assay could require days of treatment to allow for the methylated substrates to turnover.

Recently, we circumvented this problem by using human embryonic kidney 293 cells (HEK293) to develop a PABP1 inducible cell line, that, upon treatment with tetracycline (Tet), express a FLAG-tagged form of full-length PABP1 (fPABP1, Figure 4A).[98] This tag allows the induced form of PABP1 to migrate more slowly by SDS-PAGE, thus making easy to distinguish between the endogenous PABP1 and the newly synthesized fPABP1. When fPABP1 expression is induced with Tet in the presence of a potential CARM1 modulator, the degree of fPABP1 methylation can be measured using a methyl-specific antibody against the PABP1 sequence CGAIR*-PAAPR*PPFS (where R* represents an asymmetrically dimethylated arginine residue).[98]

Therefore, a Tet-inducible 3XFLAG-tagged PABP1 (fPABP) was stably transfected into HEK293 cells and post-transfection the cells were treated for 24 h with 50 μM concentrations of selected compounds **3c** and **3g**, which had triggered the highest increase of PABP1 methylation (in vitro, Table 1, 382% and 358% activation, respectively). The antimethyl-PABP1 antibody (α-Me-PABP1) was used as methylation sensor and the anti-FLAG antibody (α-FLAG, M2) to detect the induction of fPABP1 and to show protein levels. As shown in Figure 4C, when fPABP signal intensities of lane 1 (control) are compared with those of lane 3 (treatment with **3c**) or of lane 4 (treatment with **3g**), both derivatives strongly increase the methylation of fPABP1 in cells, thus confirming the in vitro activity of the compounds as well as their cell permeability.

■ CONCLUSION

PRMT-mediated arginine methylation regulates nucleosomal remodeling, gene expression, DNA repair, RNA processing and shuttling, and other cellular processes, thus the development of small molecule modulators of PRMT activity is a lively research endeavor in the field of epigenetics. Such molecules will be

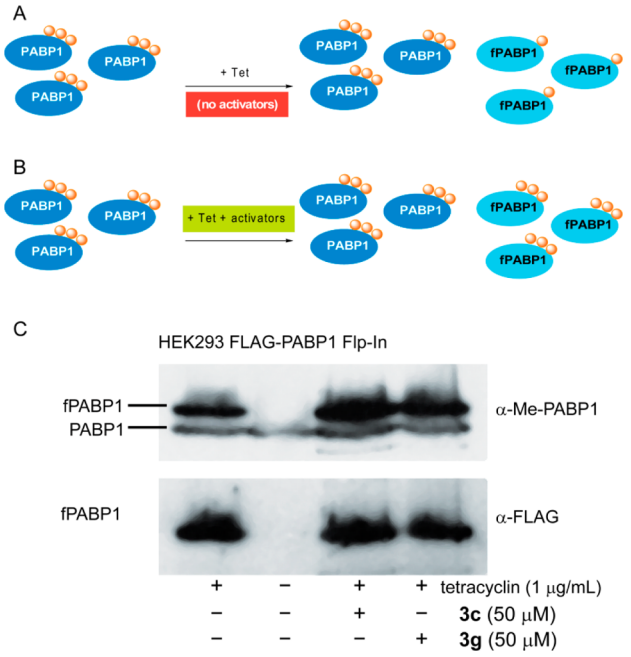

Figure 4. Effects of compounds **3c** and **3g** on arginine methylation of induced fPABP1. (A,B) The depiction of a cell-based reporter system for CARM1 activity. HEK293 cells were stably transfected with a Tet-inducible 3XFLAG-tagged PABP1 (fPABP). Orange dots represent arginine methylation on both endogenous PABP1 (sky blue) and induced fPABP1 (cyan). (A) Low levels of methylation are observed when induction takes place in the absence of activators. (B) Higher levels of methylation are observed with fPABP1 when induction takes place in the presence of an activator. (C) The fPABP1 was induced with tetracycline (1 μg/mL) in the presence of compounds **3c** or **3g** at 50 μM. The degree of methylated PABP1 was gauged by using a methyl-specific anti-PABP1 antibody (top panel). The anti-FLAG antibody (α-FLAG, M2) was used to detect the induction of fPABP1 as well as protein levels (bottom panel).

invaluable tools to study the function of protein arginine methylation and the pathways in which PRMTs are involved. After replacing the hydroxynaphthalene moiety contained in selective PRMT inhibitors previously identified by us[75,78,92] with the bioisosteric indole framework, with the aim to obtain a more versatile and synthetically handy scaffold for the future development of more potent inhibitors, we prepared 2-carboxy- and 3-carboxy-substituted indole derivatives **1a–l** and **2a–h**, respectively. We noticed that ethyl 5-(2-(3-(4-nitrophenyl)-ureido)acetamido)-1*H*-indole-2-carboxylate **1k** was endowed with an hitherto unobserved marked and dose–dependent activating effect against CARM1. Therefore, we prepared a series of ureidoacetamido indole derivatives **3a–j**, structurally related to **1k**, and found that nearly all of them increased CARM1 induced arginine methylation in vitro. We dubbed these compounds "uracandolates" (ureidoacetamido indole-2-carboxylates). The activity of the two most potent derivatives, namely **3c** and **3g**, was also confirmed in a cellular assay. Again, the simple formal shift of the carboxy function from the position 2 to position 3 of the indole ring significantly affected the activity, as the resulting derivatives **4a–l** were consistently less potent as activators or even displayed an inhibitory effect. Interestingly, a few derivatives exhibited significant differences in potency or in the activity profile when histone or nonhistone substrates were used. Such differences could be attributed to a number of possible reasons. For example, if each substrate approaches the enzyme catalytic site from a different direction, the binding of the tested compounds could differently affect substrate recognition. Otherwise, derivatives could bind to an allosteric site, thus promoting a conformational change of the enzyme structure resulting in the stabilization of a more active state but with different affinity for the two substrates, in accordance with the Monod–Wyman–Changeux (MWC) model.[118,119] Moreover, Zheng and co-workers recently published a very insightful work in which they report that a series of naphthalene-sulfo derivatives (NS), bearing structural similarities with AMI-1, directly target H4(1–20) and GAR peptide substrates instead of PRMT1, and the binding subsequently blocks the recognition of the substrates by the enzyme, which is largely responsible for the observed PRMT1 inhibition effect.[87] With the aim to investigate if tested compounds could (at least partially) recognize and directly bind specific sequences on the substrates themselves, thus enhancing or impairing their molecular recognition by the enzyme catalytic site, we performed a surface plasmon resonance-based (SPR-based) analysis of the interactions of derivatives **1k**, **3c**, **3g**, and **4e** with the enzyme, the substrate (both histone and nonhistone) peptide, and the ternary complex CARM1/substrate/SAH. We found that no interaction occur when the compounds are injected on the surface of the substrates or of the enzyme, even in the presence of SAH. Nonetheless, all the molecules significantly affect the affinity of H3 or PABP1 to CARM1/SAH complex. Moreover, we found that AMI-1 binds to CARM1 as well as to H3, whereas no binding interaction with PABP1 is detectable. Therefore, the inhibition of CARM1 activity showed by this molecule[75] may be not completely due to an interaction with the substrate as proposed,[87] at least when PABP1 is used as a substrate.

On the basis of the outcomes of the SPR analysis, it is possible to rule out the direct interaction of uracandolates with the substrates. Similarly, their negligible binding to the full-length enzyme suggests an allosteric interaction as unlikely. As a matter of fact, the mechanism underlying their biological effects remains unclear, in particular for the compounds exhibiting remarkable differences in potency or in the activity profile when histone or nonhistone substrates were used. A possible hypothesis could be that the binding of the substrate (and maybe also of the cofactor) induce structural changes allowing the binding of uracandolates, which affect methylation. Ongoing additional experiments will shed more light on this issue.

In conclusion, in this study we found that the methylation activity of CARM1 is enhanced by a series of aryl ureido acetamido indole carboxylates, both in in vitro and cellular settings. To the best of our knowledge, this is the first report of compounds acting as activators of CARM1-induced methylation.[120] While most chemical biology and drug discovery efforts are focused on identifying small molecules that inhibit enzyme function, it is quite infrequent to come across enzyme activators, yet there are significant advantages to finding them. Enzyme activators can serve as gain-of-function reagents that can be used to interrogate the biological roles of PRMTs in cells and in vivo. These activators could be used in combination with inhibitors to identify new substrates. Also, CARM1 activators may simulate the effects of CARM1 overexpression that is seen in cancer cells, and these compounds could possibly promote cellular transformation. Furthermore, it has recently been reported that the enzymatic activity of CARM1 is crucial

dx.doi.org/10.1021/jm301097p | J. Med. Chem. 2012, 55, 9875–9890

for endochondral ossification and chondrocyte proliferation,[51] for the control of myogenesis,[52] for glycogen metabolism,[53] for proper control of proliferation and differentiation of pulmonary epithelial cells,[54] and that CARM1 as well as other PRMTs (namely PRMT1 and PRMT5) are downregulated in senescent tissues.[50] Therefore, small molecules able to enhance the catalytic activity of CARM1 could be useful chemical tools for the mechanistic study of arginine methylation and its implications in physiological and/or pathological processes.

EXPERIMENTAL SECTION

Chemistry. All chemicals were purchased from Aldrich Chimica (Milan, Italy) or from Alfa Aesar GmbH (Karlsruhe, Germany) and were of the highest purity. All solvents were reagent grade and, when necessary, were purified and dried by standard methods. All reactions requiring anhydrous conditions were conducted under a positive atmosphere of nitrogen in oven-dried glassware. Standard syringe techniques were used for anhydrous addition of liquids. Reactions were routinely monitored by TLC performed on aluminum-backed silica gel plates (Merck DC, Alufolien Kieselgel 60 F254) with spots visualized by UV light (λ = 254, 365 nm) or using a $KMnO_4$ alkaline solution. Solvents were removed using a rotary evaporator operating at a reduced pressure of ~10 Torr. Organic solutions were dried over anhydrous Na_2SO_4. Chromatographic separations were performed on silica gel (silica gel 60, 0.015−0.040 mm; Merck DC) columns. Melting points were determined on a Stuart SMP30 melting point apparatus in open capillary tubes and are uncorrected. Infrared (IR) spectra (KBr) were recorded on a Shimadzu IR Affinity-1 FTIR spectrophotometer at room temperature. ^{1}H NMR spectra were recorded at 300 MHz on a Bruker Avance 300 spectrometer. Chemical shifts are reported in δ (ppm) relative to the internal reference tetramethylsilane (TMS). Mass spectra were recorded on a Finnigan LCQ DECA TermoQuest (San Jose, USA) mass spectrometer in electrospray positive and negative ionization modes (ESI-MS). Purity of tested compounds was established by combustion analysis, confirming a purity ≥95%. Elemental analyses (C, H, N) were performed on a Perkin-Elmer 2400 CHN elemental analyzer at the laboratory of microanalysis of the Department of Chemistry and Biology, University of Salerno (Italy); the analytical results were within ±0.4% of the theoretical values. When the elemental analysis is not included, compounds were used in the next step without further purification.

The synthesis of 2,5-disubstituted indole derivatives **1a**−**j** as well as of 3,5-substituted analogues **2a**−**h** is reported in Supporting Information.

*Synthesis of Ethyl 5-(2-((tert-Butoxycarbonyl)amino)acetamido)-1H-indole-2-carboxylate (**11**).* A solution of HOBt (347 mg; 2.57 mmol), HBTU (974 mg, 2.57 mmol), Boc-Gly-OH (375 mg, 2.14 mmol), and DIEA (0,90 mL; 5.14 mmol) in dry THF−DMF (7:2, 9 mL) was added to a solution of ethyl 5-amino-1*H*-indole-2-carboxylate (436 mg, 2.14 mmol) in dry THF (3 mL) under N_2 atmosphere. The reaction was stirred at room temperature overnight and then concentrated in vacuo. The residue was dissolved in EtOAc (100 mL) and washed with $NaHCO_3$ saturated aqueous solution (3 × 30 mL), citric acid 10% aqueous solution (3 × 30 mL), and brine. The organic solution was dried (Na_2SO_4), filtered, and concentrated in vacuo. The residue was purified by silica gel chromatography (EtOAc/hexanes, 7:3) to give the title compound as a white solid (626 mg, 81%); mp 193−194 °C. ^{1}H NMR (300 MHz, DMSO-d_6): δ 11.78 (s, 1H exchangeable with deuterium oxide), 9.78 (s, 1H exchangeable with deuterium oxide), 7.98 (s, 1H), 7.38−7.33 (m, 2H), 7.08 (d, 1H, J = 2.1 Hz), 6.99 (br t, 1H, J = 6.0 Hz, exchangeable with deuterium oxide), 4.31 (q, 2H, J = 7.1 Hz), 3.70 (d, 2H, J = 6.0 Hz), 1.38 (s, 9H), 1.32 (t, 3H, J = 7.1 Hz). ESI-MS m/z: 362 $(M + H)^+$.

*Synthesis of Ethyl 5-(2-(3-(4-Nitrophenyl)ureido)acetamido)-1H-indole-2-carboxylate (**1k**).* A mixture of TFA and CH_2Cl_2 (1:3, 12 mL) was added to compound **11** (300 mg, 0.83 mmol), and the reaction was stirred at room temperature for 30 min. Vacuum evaporation of the solvents gave a white solid, which was directly used in the next step. A solution of 4-nitrophenyl isocyanate (163 mg, 0.99 mmol) in dry THF (8 mL) was added dropwise to a solution of deprotected compound **11** (308 mg, 0.82 mmol) and triethylamine (0.34 mL, 2.46 mmol) in dry THF (20 mL) under N_2 atmosphere. The reaction was stirred at room temperature for 3 h. The precipitate was collected by filtration and rinsed with water and diethyl ether successively. Purification by crystallization (DMF/H_2O) gave the title compound as a white solid (244 mg, 70%); mp 290−291 °C. IR (KBr): ν = 3375, 3329, 2978, 1695, 1659, 1597, 1551, 1533 cm^{-1}. ^{1}H NMR (300 MHz, DMSO-d_6): δ 11.84 (s, 1H, exchangeable with deuterium oxide), 9.99 (s, 1H, exchangeable with deuterium oxide), 9.74 (s, 1H, exchangeable with deuterium oxide), 8.18 (d, 2H, J = 9.1 Hz), 8.02 (s, 1H), 7.67 (d, 2H, J = 9.1 Hz), 7.43−7.36 (m, 2H), 7.14−7.11 (m, 1H), 6.84 (br t, 1H, J = 5.0 Hz, exchangeable with deuterium oxide), 4.35 (q, 2H, J = 7.0 Hz), 3.99 (d, 2H, J = 5.0 Hz), 1.35 (t, 3H, J = 7.0 Hz). ESI-MS m/z: 426 $(M + H)^+$. Anal. ($C_{20}H_{19}N_5O_6$) C, H, N.

*Synthesis of 5-(2-(3-(4-Nitrophenyl)ureido)acetamido)-1H-indole-2-carboxylic Acid (**1l**).* NaOH (376 mg, 9.40 mmol) and pyridine (0.15 mL, 1.88 mmol) were added to a solution of ester **1k** (200 mg, 0.47 mmol) in THF−H_2O (4:1, 40 mL). The reaction was stirred at room temperature overnight and then concentrated in vacuo. The residue was dissolved in water (20 mL), washed with CH_2Cl_2 (3 × 10 mL), and acidified to pH 2 with 12N HCl. The precipitate was collected by filtration and washed with water. Purification by crystallization (DMF/H_2O) gave the title compound as a white solid (168 mg, 90%); mp 283−284 °C (decomp). IR (KBr): ν = 3404, 3348, 3283, 3080, 1684, 1645, 1610, 1544, 1521 cm^{-1}. ^{1}H NMR (300 MHz, DMSO-d_6): δ 11.71 (s, 1H, exchangeable with deuterium oxide), 9.98 (s, 1H, exchangeable with deuterium oxide), 9.67 (s, 1H, exchangeable with deuterium oxide), 8.18 (d, 2H, J = 9.0 Hz), 8.00 (s, 1H), 7.67 (d, 2H, J = 9.0 Hz), 7.40−7.33 (m, 2H), 7.06 (s, 1H), 6.74−6.73 (m, 1H, exchangeable with deuterium oxide), 4.00 (d, 2H, J = 4.9 Hz), the carboxylic acid proton could not be detected. ESI-MS m/z: 396 $(M - H)^-$. Anal. ($C_{18}H_{15}N_5O_6$) C, H, N.

*Synthesis of Methyl 5-Nitro-1H-indole-3-carboxylate (**7**).* Oxalyl chloride (8.52 mL, 98.7 mmol) was added dropwise to a solution of 5-nitroindole (2.00 g, 12.3 mmol) in dry EtOEt (150 mL) at 0 °C under N_2 atmosphere, and the resulting mixture was stirred at room temperature overnight. The yellow precipitate was collected by filtration, washed with cold diethyl ether, and dissolved in water (80 mL). KOH (3.25 g, 58.0 mmol) was added portionwise, and the reaction was heated to reflux for 2 h. The reaction solution was ice-cooled and acidified to pH 1 with HCl 12N. The precipitate was collected by filtration, washed with HCl 1N, and dried under vacuum. The solid was then resuspended in 10% hydrogen peroxide aqueous solution (150 mL) and heated to reflux for 4h. Resulting white precipitate was collected by filtration, washed with cold water, and dried under vacuum to give 5-nitro-1*H*-indole-3-carboxylic acid (2.27 g, 95% over two steps), which was used in the esterification step without further purification. Spectroscopic data of the title compound are consistent with those reported in the literature.[105] Sulphuric acid (1 mL) was added to a solution of 5-nitro-1*H*-indole-3-carboxylic acid (2.27 g, 11.0 mmol) in methanol (150 mL). The reaction was heated at reflux for 6 h and then concentrated in vacuo. The residue was dissolved in water, basified to pH 8 with $NaHCO_3$ saturated solution, and extracted with EtOAc (3 × 80 mL). The combined organic layers were washed with brine, dried (Na_2SO_4), filtered, and concentrated in vacuo. The crude compound was recrystallized from methanol yielding a light-yellow solid (2.18 mg, 90%); mp 288−289 °C (lit. 282−284 °C).[105] ^{1}H NMR (300 MHz, DMSO-d_6): δ 12.59 (br s, 1H, exchangeable with deuterium oxide), 8.88 (d, 1H, J = 2.2 Hz), 8.39 (s, 1H), 8.13 (dd, 1H, J = 9.0, 2.2 Hz), 7.70 (d, 1H, J = 9.0 Hz), 3.88 (s, 3H). ESI-MS m/z: 221 $(M + H)^+$.

*Synthesis of tert-Butyl 5-Nitro-1H-indole-3-carboxylate (**7′**).* 5-Nitro-1*H*-indole-3-carboxylic acid (0.500 g, 2.42 mmol), TEA (1.01 mL, 7.26 mmol), *tert*-butanol (3.40 mL, 36.3 mmol), and DCC (1.50 g, 7.26 mmol) were dissolved in dry DMF (5 mL) under N_2 atmosphere. The vessel was sealed, and the reaction was stirred at 120 °C for 3 h and then concentrated in vacuo. The residue was dissolved in EtOAc (100 mL) and washed with $NaHCO_3$ saturated

dx.doi.org/10.1021/jm301097p | J. Med. Chem. 2012, 55, 9875−9890

aqueous solution (3 × 60 mL) and brine. The organic solution was dried (Na_2SO_4), filtered, and concentrated in vacuo. The residue was purified by silica gel chromatography (CH_2Cl_2/EtOAc, 9:1) to give the title compound as a light-brown solid (585 mg, 92%); mp 212−213 °C. ^{1}H NMR (300 MHz, DMSO-d_6): δ 9.11 (s, 1H, exchangeable with deuterium oxide), 8.86 (s, 1H), 8.18 (dd, 1H, J = 8.9, 2.1 Hz), 8.01 (d, 1H, J = 2.1 Hz), 7.46 (d, 1H, J = 8.9 Hz), 1.67 (s, 9H). ESI-MS m/z: 261 $(M + H)^+$.

*Synthesis of Methyl 5-Amino-1H-indole-3-carboxylate (**8**).* Pd/C (5 wt % on activated carbon, 0.1 equiv) was added to a solution of **7** (500 mg, 2.27 mmol) in EtOH (100 mL), and the reaction was stirred under H_2 (1 atm, balloon) for 2 h. The reaction mixture was filtered and concentrated to give the title compound as a light-yellow solid (427 mg, 99%); mp 144−146 °C. ^{1}H NMR (300 MHz, DMSO-d_6): δ 11.49 (s, 1H, exchangeable with deuterium oxide), 7.82 (s, 1H), 7.17 (d, 1H, J = 2.2 Hz), 7.13 (d, 1H, J = 9.0 Hz), 6.55 (dd, 1H, J = 9.0, 2.2 Hz), 4.74 (br s, 2H, exchangeable with deuterium oxide), 3.75 (s, 3H). ESI-MS m/z: 191 $(M + H)^+$.

*Synthesis of tert-Butyl 5-Amino-1H-indole-3-carboxylate (**8′**).* Compound **8′** was obtained as a light-yellow solid (420 mg, 95%) from compound **7′** (500 mg; 1.90 mmol) according to the procedure used for **8**; mp 61−63 °C. ^{1}H NMR (300 MHz, DMSO-d_6): δ 11.62 (s, 1H, exchangeable with deuterium oxide), 8.32 (s, 1H), 7.90 (d, 1H, J = 2.1 Hz), 7.62 (br s, 2H, exchangeable with deuterium oxide), 7.36 (d, 1H, J = 9.0 Hz), 6.93−6.87 (m, 1H), 1.56 (s, 9H). ESI-MS m/z: 233 $(M + H)^+$.

*Synthesis of Ethyl 5-(2-((tert-Butoxycarbonyl)amino)acetamido)-1H-indole-3-carboxylate (**12**).* Compound **12** was obtained as a white solid (462 mg, 70%) from compound **8** (631 mg, 1.90 mmol), according to the procedure used for **11** (vide supra); mp 218−220 °C. ^{1}H NMR (300 MHz, DMSO-d_6): δ 11.85 (s, 1H, exchangeable with deuterium oxide), 9.85 (s, 1H, exchangeable with deuterium oxide), 8.22 (s, 1H), 8.03 (d, 1H, J = 2.3 Hz), 7.46 (dd, 1H, J = 8.8, 2.3 Hz), 7.39 (d, 1H, J = 8.8 Hz), 7.01 (br t, 1H, J = 6.0 Hz, exchangeable with deuterium oxide), 3.79 (s, 3H), 3.73 (d, 2H, J = 6.0 Hz), 1.41 (s, 9H). ESI-MS m/z: 348 $(M + H)^+$.

*Synthesis of tert-Butyl 5-(2-(((((9H-Fluoren-9-yl)methoxy)carbonyl)amino)acetamido)-1H-indole-3-carboxylate (**13**).* Compound **13** was obtained as a white solid (680 mg, 70%) from compound **8′** (442 mg, 1.90 mmol), according to the procedure used for **11** (vide supra) except that Fmoc-Gly-OH was used in place of Boc-Gly-OH; mp 95−96 °C. ^{1}H NMR (300 MHz, DMSO-d_6): δ 11.75 (s, 1H, exchangeable with deuterium oxide), 9.85 (s, 1H, exchangeable with deuterium oxide), 8.32 (s, 1H), 7.91−7.88 (m, 3H), 7.77−7.73 (m, 2H), 7.66−7.62 (m, 1H), 7.45−7.31 (m, 6H, one exchangeable with deuterium oxide), 4.32−4.26 (m, 3H), 3.81 (d, 2H, J = 6.0 Hz), 1.59 (s, 9H). ESI-MS m/z: 534 $(M + Na)^+$, 550 $(M + K)^+$.

*Synthesis of Ethyl 5-(2-(3-Phenylureido)acetamido)-1H-indole-2-carboxylate (**3a**).* Compound **3a** was obtained as a white solid (236 mg, 75%) from compound **11** (300 mg, 0.83 mmol) and the proper phenyl isocyanate, according to the procedure used for **1k** (vide supra); mp 263−264 °C (decomp). IR (KBr): ν = 3380, 3318, 2981, 1694, 1663, 16356, 1598, 1556, 1532 cm^{-1}. ^{1}H NMR (300 MHz, DMSO-d_6): δ 11.81 (s, 1H, exchangeable with deuterium oxide), 9.94 (s, 1H, exchangeable with deuterium oxide), 8.82 (s, 1H, exchangeable with deuterium oxide), 7.99 (s, 1H), 7.41−7.38 (m, 4H), 7.25−7.20(m, 2H), 7.10 (s, 1H), 6.92−6.87 (m, 1H), 6.43 (br t, 1H, J = 5.1 Hz, exchangeable with deuterium oxide), 4.36 (q, 2H, J = 7.0 Hz), 3.94 (d, 2H, J = 5.1 Hz), 1.35 (t, 3H, J = 7.0 Hz). ESI-MS m/z: 381 $(M + H)^+$, 403 $(M + Na)^+$. Anal. ($C_{20}H_{20}N_4O_4$) C, H, N.

*Synthesis of 5-(2-(3-Phenylureido)acetamido)-1H-indole-2-carboxylic Acid (**3b**).* Compound **3b** was obtained as a white solid (189 mg, 93%) from compound **3a** (220 mg, 0.58 mmol), according to the procedure used for **1l** (vide supra); mp 252−254 °C (decomp). IR (KBr): ν = 3379, 3298, 3057, 1694, 1670, 1627, 1595, 1541 cm^{-1}. ^{1}H NMR (300 MHz, DMSO-d_6): δ 11.68 (s, 1H, exchangeable with deuterium oxide), 9.93(s, 1H, exchangeable with deuterium oxide), 8.84 (s, 1H, exchangeable with deuterium oxide), 7.98 (s, 1H), 7.41−7.35 (m, 4H), 7.25−7.20 (m, 2H), 7.05−7.03 (m, 1H), 6.92−6.87 (m, 1H), 6.48−6.45 (m, 1H, exchangeable with deuterium oxide), 3.94 (br s, 2H), the carboxylic acid proton could not be detected. ESI-MS m/z: 353 $(M + H)^+$. Anal. ($C_{18}H_{16}N_4O_4$) C, H, N.

*Synthesis of Ethyl 5-(2-(3-(p-Tolyl)ureido)acetamido)-1H-indole-2-carboxylate (**3c**).* Compound **3c** was obtained as a white solid (274 mg, 84%) from compound **11** (300 mg, 0.83 mmol) and the proper phenyl isocyanate, according to the procedure used for **1k** (vide supra); mp 267−268 °C. IR (KBr): ν = 3387, 3327, 2980, 1699, 1670, 1639, 1597, 1544, 1533 cm^{-1}. ^{1}H NMR (300 MHz, DMSO-d_6): δ 11.80 (s, 1H, exchangeable with deuterium oxide), 9.92 (s, 1H, exchangeable with deuterium oxide), 8.70 (s, 1H, exchangeable with deuterium oxide), 7.99 (s, 1H), 7.40−7.33 (m, 2H), 7.28 (d, 2H, J = 8.1 Hz), 7.11−7.08 (m, 1H),7.02 (d, 2H, J = 8.1 Hz), 6.37 (br t, 1H, J = 5.1 Hz, exchangeable with deuterium oxide), 4.36 (q, 2H, J = 7.0 Hz), 3.93 (d, 2H, J = 5.1 Hz), 2.21 (s, 3H), 1.35 (t, 3H, J = 7.0 Hz). ESI-MS m/z: 395 $(M + H)^+$, 417 $(M + Na)^+$. Anal. ($C_{21}H_{22}N_4O_4$) C, H, N.

*Synthesis of 5-(2-(3-(p-Tolyl)ureido)acetamido)-1H-indole-2-carboxylic Acid (**3d**).* Compound **3d** was obtained as a white solid (187 mg, 96%) from compound **3c** (210 mg, 0.53 mmol), according to the procedure used for **1l** (vide supra); mp 242−244 °C (decomp). IR (KBr): ν = 3453, 3319, 3265, 3072, 1707, 1670, 1654, 1599, 1560, 1541 cm^{-1}. ^{1}H NMR (300 MHz, DMSO-d_6): δ 11.80 (s, 1H exchangeable with deuterium oxide), 9.92 (s, 1H exchangeable with deuterium oxide), 8.70 (s, 1H exchangeable with deuterium oxide), 7.99 (s, 1H), 7.40−7.33 (m, 2H), 7.28 (d, 2H, J = 8.1 Hz), 7.04−7.01 (m, 3H), 6.38−6.36 (m, 1H, exchangeable with deuterium oxide), 3.93 (d, 2H, J = 4.8 Hz), 2.21 (s, 3H), the carboxylic acid proton could not be detected. ESI-MS m/z: 367 $(M + H)^+$, 389 $(M + Na)^+$. Anal. ($C_{19}H_{18}N_4O_4$) C, H, N.

*Synthesis of Ethyl 5-(2-(3-(4-Methoxyphenyl)ureido)acetamido)-1H-indole-2-carboxylate (**3e**).* Compound **3e** was obtained as a white solid (262 mg, 77%) from compound **11** (300 mg, 0.83 mmol) and the proper phenyl isocyanate, according to the procedure used for **1k** (vide supra); mp 253−254 °C. IR (KBr): ν = 3377, 3325, 2995, 1692, 1665, 1638, 1597, 1545, 1533 cm^{-1}. ^{1}H NMR (300 MHz, DMSO-d_6): δ 11.80 (s, 1H, exchangeable with deuterium oxide), 9.91(s, 1H, exchangeable with deuterium oxide), 8.61 (s, 1H, exchangeable with deuterium oxide), 7.99 (s, 1H), 7.40−7.37 (m, 2H), 7.30 (d, 2H, J = 8.8 Hz), 7.12−7.09 (m, 1H), 6.81 (d, 2H, J = 8.8 Hz), 6.31 (br t, 1H, J = 5.0 Hz, exchangeable with deuterium oxide), 4.36 (q, 2H, J = 7.0 Hz), 3.93 (d, 2H, J = 5.0 Hz), 3.69 (s, 3H), 1.35 (t, 3H, J = 7.0 Hz). ESI-MS m/z: 411$(M + H)^+$. Anal. ($C_{21}H_{22}N_4O_5$) C, H, N.

*Synthesis of 5-(2-(3-(4-Methoxyphenyl)ureido)acetamido)-1H-indole-2-carboxylic Acid (**3f**).* Compound **3f** was obtained as a white solid (223 mg, 96%) from compound **3e** (250 mg, 0.61 mmol), according to the procedure used for **1l** (vide supra); mp 260−262 °C (decomp). IR (KBr): ν = 3399, 3321, 3267, 3096, 1670, 1654, 1603, 1541, 1508 cm^{-1}. ^{1}H NMR (300 MHz, DMSO-d_6): δ 11.67 (s, 1H, exchangeable with deuterium oxide), 9.89 (s, 1H, exchangeable with deuterium oxide), 8.61 (s, 1H, exchangeable with deuterium oxide), 7.98 (s, 1H), 7.38−7.35 (m, 2H), 7.30 (d, 2H, J = 8.8 Hz), 7.03 (s, 1H), 6.81 (d, 2H, J = 8.8 Hz), 6.34−6.31 (m, 1H exchangeable with deuterium oxide), 3.93 (d, 2H, J = 4.7 Hz), 3.69 (s, 3H), the carboxylic acid proton could not be detected. ESI-MS m/z: 383 $(M + H)^+$. Anal. ($C_{19}H_{18}N_4O_5$) C, H, N.

*Synthesis of Ethyl 5-(2-(3-(4-Cyanophenyl)ureido)acetamido)-1H-indole-2-carboxylate (**3g**).* Compound **3g** was obtained as a white solid (242 mg, 72%) from compound **11** (300 mg, 0.83 mmol) and the proper phenyl isocyanate, according to the procedure used for **1k** (vide supra); mp 279−280 °C (decomp). IR (KBr): ν = 3375, 3280, 2985, 2222, 1700, 1669, 1595, 1551, 1533 cm^{-1}. ^{1}H NMR (300 MHz, DMSO-d_6): δ 11.80 (s, 1H, exchangeable with deuterium oxide), 9.95 (s, 1H, exchangeable with deuterium oxide), 9.38 (s, 1H, exchangeable with deuterium oxide), 7.99 (s, 1H), 7.67 (d, 2H, J = 8.6 Hz), 6.58 (d, 2H, J = 8.6 Hz), 7.38−7.37 (m, 2H), 7.11−7.08 (m, 1H), 6.64 (br t, 1H, J = 5.0 Hz, exchangeable with deuterium oxide), 4.36 (q, 2H, J = 7.0 Hz), 3.97 (d, 2H, J = 5.0 Hz), 1.35 (t, 3H, J = 7.0 Hz). ESI-MS m/z: 406 $(M + H)^+$. Anal. ($C_{21}H_{19}N_5O_4$) C, H, N.

*Synthesis of 5-(2-(3-(4-Cyanophenyl)ureido)acetamido)-1H-indole-2-carboxylic Acid (**3h**).* Compound **3h** was obtained as a white

solid (173 mg, 93%) from compound **3g** (200 mg, 0.49 mmol), according to the procedure used for **1l** (vide supra); mp 269−270 °C (decomp). IR (KBr): ν = 3352, 3291, 3107, 2960, 2216, 1690, 1643, 1591, 1533 cm^{-1}. ^1H NMR (300 MHz, DMSO-d_6): δ 11.68 (s, 1H, exchangeable with deuterium oxide), 9.94(s, 1H, exchangeable with deuterium oxide), 9.39 (s, 1H, exchangeable with deuterium oxide), 7.97 (s, 1H), 7.67 (d, 2H, J = 8.6 Hz), 6.58 (d, 2H, J = 8.6 Hz), 7.38−7.31 (m, 2H), 7.04 (s, 1H), 6.64 (br t, 1H, J = 4.9 Hz, exchangeable with deuterium oxide), 3.97 (d, 2H, J = 4.9 Hz), the carboxylic acid proton could not be detected. ESI-MS m/z: 378 $(M + H)^+$. Anal. ($C_{19}H_{15}N_5O_4$) C, H, N.

*Synthesis of Ethyl 5-(2-(3-(4-(Dimethylamino)phenyl)ureido)-acetamido)-1H-indole-2-carboxylate (**3i**).* Compound **3g** was obtained as a white solid (250 mg, 71%) from compound **11** (300 mg, 0.83 mmol) and the proper phenyl isocyanate, according to the procedure used for **1k** (vide supra); mp 252−253 °C (decomp). IR (KBr): ν = 3323, 3264, 2984, 1709, 1659, 1597, 1566, 1535 cm^{-1}. ^1H NMR (300 MHz, DMSO-d_6): δ 11.70 (s, 1H, exchangeable with deuterium oxide), 9.90 (s, 1H, exchangeable with deuterium oxide), 8.45 (s, 1H, exchangeable with deuterium oxide), 7.99 (s, 1H), 7.43−7.33 (m, 2H), 7.22 (d, 2H, J = 9.0 Hz), 7.09 (s, 1H), 6.66 (d, 2H, J = 9.0 Hz), 6.29 (br t, 1H, J = 5.4 Hz, exchangeable with deuterium oxide), 4.32 (q, 2H, J = 7.0 Hz), 3.90 (d, 2H, J = 5.4 Hz), 2.80 (s, 6H), 1.33 (t, 3H, J = 7.0 Hz). ESI-MS m/z: 424 $(M + H)^+$. Anal. ($C_{22}H_{25}N_5O_4$) C, H, N.

*Synthesis of 5-(2-(3-(4-(Dimethylamino)phenyl)ureido)-acetamido)-1H-indole-2-carboxylic Acid (**3j**).* Compound **3j** was obtained as a white solid (181 mg, 81%) from compound **3i** (240 mg, 0.57 mmol), according to the procedure used for **1l** (vide supra); mp 241−243 °C (decomp). IR (KBr): ν = 3505, 3370, 3294, 2932, 1701, 1670, 1654, 1611, 1544 cm^{-1}. ^1H NMR (300 MHz, DMSO-d_6): δ 11.69 (s, 1H, exchangeable with deuterium oxide), 9.95 (s, 1H, exchangeable with deuterium oxide), 9.15 (s, 1H, exchangeable with deuterium oxide), 7.99 (s, 1H), 7.55−7.45 (m, 4H), 7.39−7.32 (m, 2H), 7.04−7.02 (m, 1H), 6.54 (br t, 1H, J = 4.8 Hz, exchangeable with deuterium oxide), 3.94 (d, 2H, J = 4.8 Hz), 3.07 (s, 6H), the carboxylic acid proton could not be detected. ESI-MS m/z: 396 $(M + H)^+$. Anal. ($C_{20}H_{21}N_5O_4$) C, H, N.

*Synthesis of Methyl 5-(2-(3-Phenylureido)acetamido)-1H-indole-3-carboxylate (**4a**).* Compound **4a** was obtained as a white solid (198 mg, 63%) from compound **12** (300 mg, 0.86 mmol) and the proper phenyl isocyanate, according to the procedure used for **1k** (vide supra); mp 260−262 °C (decomp). (KBr): ν = 3258, 3086, 2945, 1681, 1641, 1595, 1547, 1525 cm^{-1}. ^1H NMR (300 MHz, DMSO-d_6): δ 11.87 (s, 1H, exchangeable with deuterium oxide), 9.99 (s, 1H, exchangeable with deuterium oxide), 8.82 (s, 1H, exchangeable with deuterium oxide), 8.25 (s, 1H), 8.06−8.03 (m, 1H), 7.47−7.39 (m, 4H), 7.25−7.20 (m, 2H), 6.90−6.85 (m, 1H), 6.42 (br t, 1H, J = 4.9 Hz, exchangeable with deuterium oxide), 3.95 (d, 2H, J = 4.9 Hz), 3.79 (s, 3H). ESI-MS m/z: 367 $(M + H)^+$, 389 $(M + Na)^+$. Anal. ($C_{19}H_{18}N_4O_4$) C, H, N.

*Synthesis of tert-Butyl 5-(2-(3-Phenylureido)acetamido)-1H-indole-3-carboxylate (**4a′**).* Piperidine (2 mL) was added to a suspension of **13** (vide supra, 600 mg, 1.17 mmol) in CH_2Cl_2 (8 mL), and the resulting mixture was stirred at room temperature for 30 min. Vacuum evaporation of the solvent gave a solid which was washed with hexane. The white solid obtained was directly used in the next step. A solution of phenyl isocyanate (166 mg, 1.40 mmol) in dry THF (8 mL) was added dropwise to a solution of deprotected compound **13** (336 mg, 1.16 mmol) and triethylamine (0.48 mL, 3.48 mmol) in dry THF (20 mL) under N_2 atmosphere. The reaction was stirred at room temperature for 3 h. The precipitate was collected by filtration and rinsed with water and diethyl ether, successively. Purification by crystallization (DMF/H_2O) gave the title compound as a white solid (307 mg, 65%); mp 238−239 °C. (KBr): ν = 3375, 3287, 2976, 1665, 1641, 1597, 1545 cm^{-1}. ^1H NMR (300 MHz, DMSO-d_6): δ 11.76 (s, 1H, exchangeable with deuterium oxide), 9.94 (s, 1H, exchangeable with deuterium oxide), 8.82 (s, 1H, exchangeable with deuterium oxide), 8.32 (s, 1H), 7.91 (d, 1H, J = 2.5 Hz), 7.42−7.37 (m, 5H), 7.25−7.20 (m, 2H), 6.89 (br t, 1H, J = 4.9 Hz, exchangeable with deuterium oxide), 3.95 (d, 2H, J = 4.9 Hz), 1.57 (s, 9H). ESI-MS m/z: 409 $(M + H)^+$.

*Synthesis of 5-(2-(3-Phenylureido)acetamido)-1H-indole-3-carboxylic Acid (**4b**).* Compound **4b** was obtained as a white solid (112 mg, 99%) from compound **4a′** (130 mg, 0.32 mmol), according to the procedure used for **2f** (vide supra); mp 249−250 °C (decomp). IR (KBr): ν = 3387, 3311, 3213, 2934, 1676, 1662, 1595, 1551 cm^{-1}. ^1H NMR (300 MHz, DMSO-d_6): δ 11.74 (s, 1H, exchangeable with deuterium oxide), 9.96 (s, 1H, exchangeable with deuterium oxide), 8.81 (s, 1H, exchangeable with deuterium oxide), 8.24 (s, 1H), 7.95 (d, 1H, J = 2.4 Hz), 7.48−7.37 (m, 4H), 7.25−7.20 (m, 2H), 6.92−6.97 (m, 1H), 6.42 (br t, 1H, J = 5.1 Hz, exchangeable with deuterium oxide), 3.94 (d, 2H, J = 5.1 Hz), the carboxylic acid proton could not be detected. ESI-MS m/z: 353 $(M + H)^+$, 357 $(M + Na)^+$. Anal. ($C_{18}H_{16}N_4O_4$) C, H, N.

*Synthesis of Methyl 5-(2-(3-(p-Tolyl)ureido)acetamido)-1H-indole-3-carboxylate (**4c**).* Compound **4c** was obtained as a white solid (271 mg, 83%) from compound **12** (300 mg, 0.86 mmol) and the proper phenyl isocyanate, according to the procedure used for **1k** (vide supra); mp 271−273 °C (decomp). (KBr): ν = 3395, 3250, 3092, 1672, 1647, 1603, 1541, 1526 cm^{-1}. ^1H NMR (300 MHz, DMSO-d_6): δ 11.86 (s, 1H, exchangeable with deuterium oxide), 9.98 (s, 1H, exchangeable with deuterium oxide), 8.70 (s, 1H, exchangeable with deuterium oxide), 8.25 (s, 1H), 8.03 (d, 1H, J = 1.9 Hz), 7.45−7.38 (m, 2H), 7.29 (d, 2H, J = 8.1 Hz), 7.03 (d, 2H, J = 8.1 Hz), 6.38 (br t, 1H, J = 5.1 Hz, exchangeable with deuterium oxide), 3.94 (d, 2H, J = 5.1 Hz), 3.79 (s, 3H), 2.21 (s, 3H). ESI-MS m/z: 381 $(M + H)^+$, 403 $(M + Na)^+$. Anal. ($C_{20}H_{20}N_4O_4$) C, H, N.

*Synthesis of tert-Butyl 5-(2-(3-(p-Tolyl)ureido)acetamido)-1H-indole-3-carboxylate (**4c′**).* Compound **4c′** was obtained as a white solid (392 mg, 80%) from compound **13** (vide supra, 600 mg, 1.17 mmol) and the proper phenyl isocyanate, according to the procedure used for **4a′**; mp 243−245 °C. (KBr): ν = 3366, 3323, 3267, 2978, 1670, 1643, 1597, 1545 cm^{-1}. ^1H NMR (300 MHz, DMSO-d_6): δ 11.75 (s, 1H, exchangeable with deuterium oxide), 9.93 (s, 1H, exchangeable with deuterium oxide), 8.72 (s, 1H, exchangeable with deuterium oxide), 8.32 (s, 1H), 7.92−7.90 (m, 1H), 7.38−7.35 (m, 2H), 7.29 (d, 2H, J = 8.0 Hz), 7.03 (d, 2H, J = 8.0 Hz), 6.38 (br t, 1H, J = 4.9 Hz, exchangeable with deuterium oxide), 3.94 (d, 2H, J = 4.9 Hz), 2.21 (s, 3H), 1.57 (s, 9H). ESI-MS m/z: 423 $(M + H)^+$, 445 $(M + Na)^+$.

*Synthesis of 5-(2-(3-(p-Tolyl)ureido)acetamido)-1H-indole-3-carboxylic Acid (**4d**).* Compound **4d** was obtained as a white solid (120 mg, 99%) from compound **4c′** (140 mg, 0.33 mmol), according to the procedure used for **2f** (vide supra); mp 219−221 °C (decomp). IR (KBr): ν = 3372, 3282, 3117, 2920, 1662, 1647, 1599, 1551 cm^{-1}. ^1H NMR (300 MHz, DMSO-d_6): 11.86 (s, 1H, exchangeable with deuterium oxide), 9.95 (s, 1H, exchangeable with deuterium oxide), 8.70 (s, 1H, exchangeable with deuterium oxide), 8.24 (s, 1H), 7.96 (d, 1H, J = 2.6 Hz), 7.46 (d, 1H, J = 9.6 Hz), 7.38−7.35 (m, 1H), 7.28 (d, 2H, J = 8.2 Hz), 7.03 (d, 2H, J = 8.2 Hz), 6.38 (br t, 1H, J = 5.2 Hz, exchangeable with deuterium oxide), 3.94 (d, 2H, J = 5.2 Hz), 2.21 (s, 3H), the carboxylic acid proton could not be detected. ESI-MS m/z: 367 $(M + H)^+$, 389 $(M + Na)^+$. Anal. ($C_{19}H_{18}N_4O_4$) C, H, N.

*Synthesis of Methyl 5-(2-(3-(4-Methoxyphenyl)ureido)-acetamido)-1H-indole-3-carboxylate (**4e**).* Compound **4e** was obtained as a white solid (276 mg, 81%) from compound **12** (300 mg, 0.86 mmol) and the proper phenyl isocyanate, according to the procedure used for **1k** (vide supra); mp 250−252 °C (decomp). (KBr): ν = 3389, 3285, 3080, 1680, 1639, 1599, 1554 cm^{-1}. ^1H NMR (300 MHz, DMSO-d_6): δ 11.85 (s, 1H, exchangeable with deuterium oxide), 9.96 (s, 1H, exchangeable with deuterium oxide), 8.61 (s, 1H, exchangeable with deuterium oxide), 8.25 (s, 1H), 8.03 (d, 1H, J = 2.6 Hz), 7.45−7.40 (m, 2H), 7.30 (d, 2H, J = 8.6 Hz), 6.82 (d, 2H, J = 8.6 Hz), 6.32 (br t, 1H, J = 5.0 Hz, exchangeable with deuterium oxide), 3.93 (d, 2H, J = 5.0 Hz), 3.70 (s, 3H), 3.70 (s, 3H). ESI-MS m/z: 397 $(M + H)^+$, 419 $(M + Na)^+$. Anal. ($C_{20}H_{20}N_4O_5$) C, H, N.

*Synthesis of tert-Butyl 5-(2-(3-(4-Methoxyphenyl)ureido)-acetamido)-1H-indole-3-carboxylate (**4e′**).* Compound **4e′** was obtained as a white solid (343 mg, 67%) from compound **13** (vide

supra, 600 mg, 1.17 mmol) and the proper phenyl isocyanate, according to the procedure used for **4a′**; mp 238−240 °C. (KBr): ν = 3373, 3325, 3273, 2976, 1670, 1641, 1600, 1551 cm^{-1}. ^{1}H NMR (300 MHz, DMSO-d_6): δ 11.75 (s, 1H, exchangeable with deuterium oxide), 9.92 (s, 1H, exchangeable with deuterium oxide), 8.62 (s, 1H, exchangeable with deuterium oxide), 8.32 (s, 1H), 7.92−7.90 (m, 1H), 7.37−7.34 (m, 2H), 7.29 (d, 2H, J = 8.9 Hz), 6.81 (d, 2H, J = 8.9 Hz), 6.33 (br t, 1H, J = 5.4 Hz, exchangeable with deuterium oxide), 3.94 (d, 2H, J = 5.4 Hz), 3.69 (s, 3H), 1.57 (s, 9H). ESI-MS m/z: 439 (M + H)$^+$, 461 (M + Na)$^+$.

*Synthesis of 5-(2-(3-(4-Methoxyphenyl)ureido)acetamido)-1H-indole-3-carboxylic Acid (**4f**).* Compound **4f** was obtained as a white solid (112 mg, 99%) from compound **4e′** (130 mg, 0.30 mmol), according to the procedure used for **2f** (vide supra); mp 271−273 °C (decomp). IR (KBr): ν = 3366, 3282, 3012, 2933, 1670, 1654, 1609, 1541 cm^{-1}. ^{1}H NMR (300 MHz, DMSO-d_6): δ 11.74 (s, 1H, exchangeable with deuterium oxide), 9.95 (s, 1H, exchangeable with deuterium oxide), 8.61 (s, 1H, exchangeable with deuterium oxide), 8.22 (s, 1H), 7.94 (d, 1H, J = 2.6 Hz), 7.45−7.34 (m, 2H), 7.28 (d, 2H, J = 8.9 Hz), 6.80 (d, 2H, J = 8.9 Hz), 6.33 (br t, 1H, J = 5.2 Hz, exchangeable with deuterium oxide), 3.93 (d, 2H, J = 5.2 Hz), 3.69 (s, 3H), the carboxylic acid proton could not be detected. ESI-MS m/z: 381 (M − H)$^-$. Anal. ($C_{19}H_{18}N_4O_5$) C, H, N.

*Synthesis of Methyl 5-(2-(3-(4-Cyanophenyl)ureido)acetamido)-1H-indole-3-carboxylate (**4g**).* Compound **4g** was obtained as a white solid (265 mg, 79%) from compound **12** (300 mg, 0.86 mmol) and the proper phenyl isocyanate, according to the procedure used for **1k** (vide supra); mp 268−270 °C . (KBr): ν = 3370, 3273, 3113, 2232, 1672, 1645, 1591, 1551 cm^{-1}. ^{1}H NMR (300 MHz, DMSO-d_6): δ 11.86 (s, 1H, exchangeable with deuterium oxide), 10.01 (s, 1H, exchangeable with deuterium oxide), 9.39 (s, 1H, exchangeable with deuterium oxide), 8.25 (s, 1H), 8.03 (d, 1H, J = 2.5 Hz), 7.68 (d, 2H, J = 8.8 Hz), 7.59 (d, 2H, J = 8.8 Hz), 7.45−7.37 (m, 2H), 6.65 (br t, 1H, J = 5.3 Hz, exchangeable with deuterium oxide), 3.97 (d, 2H, J = 5.3 Hz), 3.79 (s, 3H). ESI-MS m/z: 392 (M + H)$^+$, 411 (M + Na)$^+$. Anal. ($C_{20}H_{17}N_5O_4$) C, H, N.

*Synthesis of tert-Butyl 5-(2-(3-(4-Cyanophenyl)ureido)-acetamido)-1H-indole-3-carboxylate (**4g′**).* Compound **4g′** was obtained as a white solid (380 mg, 75%) from compound **13** (vide supra, 600 mg, 1.17 mmol) and the proper phenyl isocyanate, according to the procedure used for **4a′**; mp 228−230 °C. (KBr): ν = 3348, 3273, 2980, 2224, 1670, 1643, 1589, 1541 cm^{-1}. ^{1}H NMR (300 MHz, DMSO-d_6): δ 11.76 (s, 1H, exchangeable with deuterium oxide), 9.96 (s, 1H, exchangeable with deuterium oxide), 9.44 (s, 1H, exchangeable with deuterium oxide), 8.31 (s, 1H), 7.92−7.90 (m, 1H), 7.97 (d, 2H, J = 8.6 Hz), 7.59 (d, 2H, J = 8.6 Hz), 7.39−7.35 (m, 2H), 6.88 (br t, 1H, J = 4.7 Hz, exchangeable with deuterium oxide), 3.97 (d, 2H, J = 4.7 Hz), 1.56 (s, 9H). ESI-MS m/z: 456 (M + Na)$^+$.

*Synthesis of 5-(2-(3-(4-Cyanophenyl)ureido)acetamido)-1H-indole-3-carboxylic Acid (**4h**).* Compound **4h** was obtained as a white solid (121 mg, 99%) from compound **4g′** (140 mg, 0.32 mmol), according to the procedure used for **2f** (vide supra); mp 238−239 °C (decomp). IR (KBr): ν = 3344, 3309, 3128, 2926, 2224, 1670, 1664, 1595, 1545 cm^{-1}. ^{1}H NMR (300 MHz, DMSO-d_6): δ 11.75 (s, 1H, exchangeable with deuterium oxide), 9.99 (s, 1H, exchangeable with deuterium oxide), 9.40 (s, 1H, exchangeable with deuterium oxide), 8.23 (s, 1H), 7.95 (d, 1H, J = 2.3 Hz), 7.68 (d, 2H, J = 8.5 Hz), 7.58 (d, 2H, J = 8.5 Hz), 7.46−7.38 (m, 2H), 6.65 (br t, 1H, J = 4.9 Hz, exchangeable with deuterium oxide), 3.95 (d, 2H, J = 4.9 Hz), the carboxylic acid proton could not be detected. ESI-MS m/z: 376 (M − H)$^-$. Anal. ($C_{19}H_{15}N_5O_4$) C, H, N.

*Synthesis of Methyl 5-(2-(3-(4-Nitrophenyl)ureido)acetamido)-1H-indole-3-carboxylate (**4i**).* Compound **4i** was obtained as a white solid (244 mg, 69%) from compound **12** (300 mg, 0.86 mmol) and the proper phenyl isocyanate, according to the procedure used for **1k** (vide supra); mp 288−290 °C (decomp). (KBr): ν = 3364, 3273, 3082, 1670, 1645, 1560 cm^{-1}. ^{1}H NMR (300 MHz, DMSO-d_6): δ 11.85 (s, 1H, exchangeable with deuterium oxide), 10.05 (s, 1H, exchangeable with deuterium oxide), 9.06 (s, 1H, exchangeable with deuterium oxide), 8.27 (s, 1H), 8.18 (d, 2H, J = 9.1 Hz), 8.06 (d, 1H, J = 2.7 Hz), 7.67 (d, 2H, J = 9.1 Hz), 7.60−7.38 (m, 2H), 7.01 (br t, 1H, J = 4.8 Hz, exchangeable with deuterium oxide), 3.73 (d, 2H, J = 4.8 Hz), 3.81 (s, 3H). ESI-MS m/z: 412 (M + H)$^+$. Anal. ($C_{19}H_{17}N_5O_6$) C, H, N.

*Synthesis of tert-Butyl 5-(2-(3-(4-Nitrophenyl)ureido)acetamido)-1H-indole-3-carboxylate (**4i′**).* Compound **4i′** was obtained as a yellow solid (377 mg, 71%) from compound **13** (vide supra, 600 mg, 1.17 mmol) and the proper phenyl isocyanate, according to the procedure used for **4a′**; mp 237−239 °C. (KBr): ν = 3368, 3271, 2980, 1676, 1647, 1597, 1551 cm^{-1}. ^{1}H NMR (300 MHz, DMSO-d_6): δ 11.76 (s, 1H, exchangeable with deuterium oxide), 9.98 (s, 1H, exchangeable with deuterium oxide), 9.65 (s, 1H, exchangeable with deuterium oxide), 8.32 (s, 1H), 8.15 (d, 2H, J = 9.0 Hz), 7.91 (d, 1H, J = 2.5 Hz), 7.65 (d, 2H, J = 9.0 Hz), 7.40−7.37 (m, 2H), 6.72 (br t, 1H, J = 5.0 Hz, exchangeable with deuterium oxide), 4.00 (d, 2H, J = 5.0 Hz), 1.57 (s, 9H). ESI-MS m/z: 476 (M + Na)$^+$.

*Synthesis of 5-(2-(3-(4-Nitrophenyl)ureido)acetamido)-1H-indole-3-carboxylic Acid (**4j**).* Compound **4j** was obtained as a yellow solid (104 mg, 99%) from compound **4i′** (120 mg, 0.26 mmol), according to the procedure used for **2f** (vide supra); mp 283−285 °C (decomp). IR (KBr): ν = 3345, 3309, 3138, 2922, 1662, 1599, 1541 cm^{-1}. ^{1}H NMR (300 MHz, DMSO-d_6): δ 11.89 (s, 1H, exchangeable with deuterium oxide), 11.75 (s, 1H, exchangeable with deuterium oxide), 10.00 (s, 1H, exchangeable with deuterium oxide), 9.63 (s, 1H), 8.16 (d, 2H, J = 9.0 Hz), 7.95 (d, 1H, J = 2.1 Hz), 7.65 (d, 2H, J = 9.0 Hz), 7.47−7.39 (m, 2H), 6.72 (br t, 1H, J = 4.8 Hz, exchangeable with deuterium oxide), 3.98 (d, 2H, J = 4.8 Hz), the carboxylic acid proton could not be detected. ESI-MS m/z: 398 (M + H)$^+$. Anal. ($C_{18}H_{15}N_5O_6$) C, H, N.

*Synthesis of Methyl 5-(2-(3-(4-(Dimethylamino)phenyl)ureido)-acetamido)-1H-indole-3-carboxylate (**4k**).* Compound **4k** was obtained as a white solid (228 mg, 65%) from compound **12** (300 mg, 0.86 mmol) and the proper phenyl isocyanate, according to the procedure used for **1k** (vide supra); mp 244−246 °C (decomp). (KBr): ν = 3289, 3118, 2945, 1668, 1630, 1525 cm^{-1}. ^{1}H NMR (300 MHz, DMSO-d_6): δ 11.85 (s, 1H, exchangeable with deuterium oxide), 9.94 (s, 1H, exchangeable with deuterium oxide), 8.41 (s, 1H, exchangeable with deuterium oxide), 8.25 (s, 1H), 8.03 (d, 1H, J = 2.1 Hz), 7.46 (dd, 1H, J = 8.8, 2.1 Hz), 7.40 (d, 1H, J = 8.8 Hz), 7.21 (d, 2H, J = 9.0 Hz), 6.66 (d, 2H, J = 9.0 Hz), 6.25 (br t, 1H, J = 5.4 Hz, exchangeable with deuterium oxide), 3.92 (d, 2H, J = 5.4 Hz), 3.79 (s, 3H), 2.80 (s, 6H). ESI-MS m/z: 432 (M + Na)$^+$. Anal. ($C_{21}H_{23}N_5O_4$) C, H, N.

*Synthesis of tert-Butyl 5-(2-(3-(4-(Dimethylamino)phenyl)-ureido)acetamido)-1H-indole-3-carboxylate (**4k′**).* Compound **4k′** was obtained as a white solid (375 mg, 71%) from compound **13** (vide supra, 600 mg, 1.17 mmol) and the proper phenyl isocyanate, according to the procedure used for **4a′**; mp 225−227 °C. (KBr): ν = 3379, 3325, 2978, 1670, 1641, 1597, 1545 cm^{-1}. ^{1}H NMR (300 MHz, DMSO-d_6): δ 11.78 (s, 1H, exchangeable with deuterium oxide), 9.92 (s, 1H, exchangeable with deuterium oxide), 8.50 (s, 1H, exchangeable with deuterium oxide), 8.32 (s, 1H), 7.90 (d, 1H, J = 2.6 Hz), 7.38−7.35 (m, 2H), 7.21 (d, 2H, J = 8.7 Hz), 6.67 (d, 2H, J = 8.7 Hz), 6.30 (br t, 1H, J = 5.2 Hz, exchangeable with deuterium oxide), 3.92 (d, 2H, J = 5.2 Hz), 2.80 (s, 6H), 1.57 (s, 9H). ESI-MS m/z: 452 (M + H)$^+$, 474 (M + Na)$^+$.

*Synthesis of 5-(2-(3-(4-(Dimethylamino)phenyl)ureido)-acetamido)-1H-indole-3-carboxylic Acid Trifluoroacetate (**4l**).* Compound **4l** was obtained as a yellow solid (113 mg, 99%) from compound **4k′** (130 mg, 0.29 mmol), according to the procedure used for **2f** (vide supra); mp 201−204 °C (decomp). IR (KBr): ν = 3356, 3310, 3246, 2960, 1668, 1654, 1597, 1555 cm^{-1}. ^{1}H NMR (300 MHz, DMSO-d_6): δ 11.88 (s, 1H, exchangeable with deuterium oxide), 10.02 (s, 1H, exchangeable with deuterium oxide), 9.33 (br s, 1H, exchangeable with deuterium oxide), 8.26 (s, 1H), 7.96−7.93 (m, 1H), 7.47−7.36 (m, 6H), 6.67 (br t, 1H, J = 4.9 Hz, exchangeable with deuterium oxide), 3.93 (d, 2H, J = 4.9 Hz), 2.37 (s, 6H), the carboxylic acid proton and the dimethylammonium salt proton could not be detected. ESI-MS m/z: 396 (M + H)$^+$. Anal. ($C_{22}H_{22}F_3N_5O_6$) C, H, N.

Biochemistry. *Plasmids, Antibodies, and Chemicals.* All GST fusion proteins were subcloned into pGEX6P-1 (Amersham Biosciences), which allows for the induced production of recombinant proteins fused to the C terminus of glutathione *S*-transferase. GST-PABP1,[31] has been previously described. GST-Npl3p was a gift from Pam Silver (Harvard Medical School, MA, USA) and has been described previously.[37] GST-SET7/9 was a gift from Yi Zhang (Lineberger Comprehensive Cancer Center, Chapel Hill, USA). GST−G9a was a gift from Yoichi Shinkai (Institute for Virus Research, Kyoto, Japan).[121] Histones H3 and H4 from calf thymus were purchased from Roche Applied Science. MBP was purchased from Sigma−Aldrich. The methyl-specific anti-PABP1 antibody against the peptide sequence CGAIR*PAAPR*PPFS from PABP1 was raised in New Zealand white rabbits. The anti-Flag antibody, M2, was purchased from Sigma−Aldrich. Unless stated otherwise, all chemicals/reagents were purchased from Sigma-Aldrich.

Preparation of GST-PRMT Fusion Proteins. Expression of the GST-PRMT1 fusion protein is described in Supporting Information.

GST-PRMT3 and GST-PRMT4 have been described previously.[122]

GST-PABP1(437−488) Expression and Purification. The construct for human PABP1 encoding residues 437 to 488, PABP1(437−488), was generated by subcloning a PCR amplified fragment from the full length PABP1 gene (a gift from Dr. Bertrand Séraphin at IGBMC) into the expression vector pGEX-2T (GE Healthcare).

Escherichia coli BL21(DE3) cells transformed with the PABP1(437−488) plasmid were grown in LB at 37 °C. The GST-fusion protein expression was induced with 0.2 mM IPTG overnight at 20 °C. Harvested cells were lysed by sonication in 50 mM Tris-HCl, pH 8.2, 200 mM NaCl. The lysate was clarified by centrifugation at 25000*g* for 30 min and applied to a 2 mL of Glutathione Sepharose 4B (GE Healthcare) column. The GST-fusion protein was eluted with two column volumes of 50 mM reduced glutathione in the lysis buffer and concentrated using an Amicon Ultra with a cutoff of 10 kDa. The concentration of 164 μM was measured by UV absorption (ε_{280} = 46370 M^{-1} cm^{-1}), and the protein was stored at −20 °C in 50 mM Tris pH 8.5, 200 mM NaCl, 0.5 mM dithiothreitol (DTT), 50% (v/v) glycerol.

Protein Methyltransferase Assays. *PRMT1, PRMT3, PRMT4/CARM1, and SET7/9 in Vitro Methylation Assays.* In vitro methylation assays were described in detail previously.[75] Briefly, all methylation reactions were carried out in the presence of [^{3}H] SAM (0.42 μM, 79 Ci/mmol, stock solution in diluted HCl/ethanol 9:1, pH 2.0−2.5, GE Healthcare) and PBS (137 mM NaCl, 2.7 mM KCl, 4.3 mM Na_2HPO_4, 1.4 mM KH_2PO_4, pH 7.4). To determine the specificity of their inhibitory activity, tested compounds were incubated with GST-PRMT1 (10×10^{-8} M) and histone H4 (all 1.5×10^{-6} M), GST-PRMT3 (9.0×10^{-8} M) and GAR (4.1×10^{-7} M), GST-PRMT4 (9.8×10^{-8} M) and histone H3 (all 1.1×10^{-6} M), and SET 7/9 (1.3×10^{-7} M) and histone H3. Histones were purchased from Roche. Substrates (0.5 μg, concentration range from 1.1×10^{-6} M to 4.06×10^{-7} M) were incubated with recombinant enzymes (0.2 μg, concentration range from 1.3×10^{-7} M to 10×10^{-8} M) in the presence of 0.5 μg of [^{3}H] SAM (0.42 μM) and 50 μM of compound for 90 min at 30 °C in a final volume of 30 μL. Reactions were run on a 10% SDS-PAGE, transferred to a polyvinylidene fluoride (PVDF) membrane (Millipore), sprayed with a spray surface autoradiography enhancer (EN^{3}HANCE, PerkinElmer), and exposed to film overnight. Band intensities were calculated using a Kodak Image Station 440 and 1D Image Analysis Software (Eastman Kodak Co.).

Surface Plasmon Resonance Analysis of Binding Interactions. SPR analyses were performed on a Biacore 3000 optical biosensor equipped with research-grade CM5 sensor chips (Biacore AB).[123] Using this platform, one peptide (PABP1(437−488)) or protein (cal thymus histone H3 or GST-PRMT4 full length) surface, one BSA surface, and one unmodified reference surface were prepared for simultaneous analyses. Proteins (30 μg mL^{-1} in 10 mM sodium acetate, pH 4.5) were immobilized on individual flow cells of the sensor chip at a flow rate of 5 mL min^{-1} by using standard amine-coupling protocols[124] to obtain densities of 12−17 kRU. Compounds **1k**, **3c**, **3g**, and **4e** as well as reference compounds AMI-1 and ellagic acid were dissolved in DMSO (100%) to obtain 50 mM solutions and diluted in HBS (10 mM Hepes pH 7.4, 0.15 M NaCl, 0.005% NP40) with a final DMSO concentration of 0.5%. For each sample, the complete binding study was performed using a six-point concentration series, typically spanning 0.025−10 μM. Binding experiments were performed using a flow rate of 50 μL min^{-1}, with 60 s monitoring of association and 300 s monitoring of dissociation. HBS or 200 μM SAH in HBS were used as running buffer. To evaluate the affinity of H3 or PABP1(437−488) toward CARM1 in the presence of derivatives **1k**, **3c**, **3g**, and **4e**, each substrate was dissolved in HBS at four different concentrations (10 nM, 50 nM, 250 nM, and 1 μM), and five aliquots of each sample were dispensed into single-use vials; each derivative was then added to a complete substrate concentration series to a final concentration of 4 μM, whereas 0.1% DMSO was added to the fifth series. Binding experiments were performed using a flow rate of 20 μL min^{-1}, with 60 s monitoring of association and 300 s monitoring of dissociation, using HBS or 200 μM SAH in HBS as running buffer. Simple interactions were adequately fit to a single-site bimolecular interaction model (A + B = AB), yielding a single K_D. Sensorgram elaborations were performed using the BIAevaluation software provided by GE Healthcare.

Cellular Methylation Assay. A stable/inducible T-Rex-3XFlag-PABP1 cell line was established by transfection with pcDNA/FRT/TO-3XFlag-PAPBP1 and pOG44 plasmids into Flp-in T-Rex HEK293 cells (Invitrogen).

Transfected cells were maintained in Dulbecco's Modified Eagle's Medium containing fetal bovine serum (10%) supplemented with blasticidin (10 μg/mL) and hygromycin (100 μg/mL). The resistant single colony was picked and propagated.

Cells were plated out in 6-well plates at a density of 1×10^5 cells/mL in DMEM media supplemented with 10% FBS. After 12 h, the media was changed. Cells were either treated with DMSO alone (negative or background control), tetracyclin alone (positive control), compound alone, or compound in combination with tetracyclin.

The final concentration of compound was 100 μM; the final concentration of tetracyclin was 1 μg/μL. After 24 h, the cells were harvested and lysed with RIPA buffer. The lysates were subsequently immunoblotted.

Quantification of CARM1 Fluorographs. Band intensities were calculated by staining the bands with Ponceau Red. The stained bands were then cut out and put in a glass vial each. Then 2 mL of a scintilization cocktail (CytoScint, MPBio) were added to each vial and the samples were counted using a Packard 1600 TR liquid scintilization analyzer. The counts of the excised area were compared to the DMSO control. This approach was used in Figure 3 and in Figure S2, Supporting Information.

Quantification of PABP1 Western Blot. The film was scanned and digitalized. The density of each band was determined using the Quantity One 1-D analysis software (Bio-Rad) and compared to the DMSO control. This approach was used in Figure 4.

■ ASSOCIATED CONTENT

Ⓢ Supporting Information

Synthesis of 2,5-disubstituted indole derivatives **1a−j** and of 3,5-substituted analogues **2a−h**, elemental analysis for all final compounds, preparation of GST-PRMT1 fusion protein, description of PRMT1 inhibitory assay, additional biological data. This material is available free of charge via the Internet at http://pubs.acs.org.

■ AUTHOR INFORMATION

Corresponding Author

*Phone: +39-089-96-9770. Fax:+39-089-96-9602. E-mail: gsbardella@unisa.it.

Present Address

#Celon Pharma Sp. Z.o.o., Laboratory of Medicinal Chemistry, ulica Ogrodowa 2A, 05−092 Lomianki/Kielpin, Poland.

Notes

The authors declare no competing financial interest.

■ ACKNOWLEDGMENTS

This work was supported by grants from Ministero dell'Università e della Ricerca Scientifica e Tecnologica, PRIN 2008 (S.C.), Università di Salerno (G.S.), COST Action TD09/05 Epigenetics (G.S. and A.M.), and NIEHS Center institutional grants ES007784, ES015188, and DK062248 (M.T.B.). A.S. was supported by a Fellowship from German Research Foundation, SP 1262/1-1. C.M. and M.V. were supported by Università di Salerno with a postdoctoral research fellowship and a predoctoral fellowship, respectively. We are indebted to Dr. Marina Fasolini (Nerviano MS) for helpful discussions.

■ ABBREVIATIONS USED

AIB1, amplified in breast cancer-1; BL21, *Escherichia coli* B cells lacking the Lon protease; BSA, bovine serum albumin; CARM1, coactivator-associated arginine methyltransferase 1; CBP, CREB binding protein; CREB, *c*-AMP response element-binding; aDMA, asymmetrical dimethylarginine; sDMA, symmetrical dimethylarginine; DTT, dithiothreitol; FBXO11, F-box protein 11; GAR, glycine-rich, arginine rich; GST, glutathione-*S*-transferase; HKMT, histone lysine methyltransferase; hnRNP, heterogeneous nuclear ribonucleoprotein; HRP, horseradish peroxidase; IPTG, isopropyl-*β*-D-1-thiogalactopyranoside; LB, lysogeny broth; MMA, monomethylarginine; NF-*κ*B, nuclear factor *κ*B; Npl3p, nuclear shuttling protein; p300, E1A binding protein 300 kDa; PABP1, polyadenylate-binding protein 1; PBS, phosphate buffer saline; PRMT, protein arginine methyl transferase; PVDF, polyvinylidene fluoride; RmtA, fungal arginine methyltransferase A; SAM, *S*-adenosyl methionine; SDS-PAGE, sodium dodecyl sulfatepolyacrylamide gel electrophoresis; SET, Su(var.) 3–9, enhancer-of-zeste and trithorax; TBS, Tris buffered saline; TBST, Tris buffered saline Tween-20; TCA, trichloroacetic acid; TFA, trifluoroacetic acid

■ REFERENCES

(1) Aletta, J. M.; Hu, J. C.; El-Gewely, M. R. Protein arginine methylation in health and disease. In *Biotechnology Annual Review*; Elsevier: New York, 2008; Vol. *14*, pp 203–224.

(2) Bedford, M. T.; Richard, S. Arginine Methylation: An Emerging Regulator of Protein Function. *Mol. Cell* **2005**, *18*, 263–272.

(3) Krause, C. D.; Yang, Z.-H.; Kim, Y.-S.; Lee, J.-H.; Cook, J. R.; Pestka, S. Protein arginine methyltransferases: evolution and assessment of their pharmacological and therapeutic potential. *Pharmacol. Ther.* **2007**, *113*, 50–87.

(4) Pahlich, S.; Zakaryan, R. P.; Gehring, H. Protein arginine methylation: cellular functions and methods of analysis. *Biochim. Biophys. Acta, Proteins Proteomics* **2006**, *1764*, 1890–1903.

(5) Bedford, M. T. Arginine methylation at a glance. *J. Cell Sci.* **2007**, *120*, 4243–4246.

(6) Smith, B. C.; Denu, J. M. Chemical mechanisms of histone lysine and arginine modifications. *Biochim. Biophys. Acta, Gene Regul. Mech.* **2009**, *1789*, 45–57.

(7) Di Lorenzo, A.; Bedford, M. T. Histone arginine methylation. *FEBS Lett.* **2011**, *585*, 2024–2031.

(8) PRMT1 and other PRMTs except PRMT4 recognize glycine arginine rich motifs for methylation, whereas PRMT4 recognizes XXPRXX motif for methylation.

(9) Bedford, M. T.; Clarke, S. G. Protein Arginine Methylation in Mammals: Who, What, and Why. *Mol. Cell* **2009**, *33*, 1–13.

(10) Miranda, T. B.; Miranda, M.; Frankel, A.; Clarke, S. PRMT7 Is a Member of the Protein Arginine Methyltransferase Family with a Distinct Substrate Specificity. *J. Biol. Chem.* **2004**, *279*, 22902–22907.

(11) Kousaka, A.; Mori, Y.; Koyama, Y.; Taneda, T.; Miyata, S.; Tohyama, M. The distribution and characterization of endogenous protein arginine *N*-methyltransferase 8 in mouse CNS. *Neuroscience* **2009**, *163*, 1146–1157.

(12) Taneda, T.; Miyata, S.; Kousaka, A.; Inoue, K.; Koyama, Y.; Mori, Y.; Tohyama, M. Specific regional distribution of protein arginine methyltransferase 8 (PRMT8) in the mouse brain. *Brain Res.* **2007**, *1155*, 1–9.

(13) Selvi, B. R.; Mohankrishna, D. V.; Ostwal, Y. B.; Kundu, T. K. Small molecule modulators of histone acetylation and methylation: A disease perspective. *Biochim. Biophys. Acta, Gene Regul. Mech.* **2010**, *1799*, 810–828.

(14) Guccione, E.; Bassi, C.; Casadio, F.; Martinato, F.; Cesaroni, M.; Schuchlautz, H.; Luscher, B.; Amati, B. Methylation of histone H3R2 by PRMT6 and H3K4 by an MLL complex are mutually exclusive. *Nature* **2007**, *449*, 933–937.

(15) Kirmizis, A.; Santos-Rosa, H.; Penkett, C. J.; Singer, M. A.; Vermeulen, M.; Mann, M.; Bahler, J.; Green, R. D.; Kouzarides, T. Arginine methylation at histone H3R2 controls deposition of H3K4 trimethylation. *Nature* **2007**, *449*, 928–932.

(16) Arrowsmith, C. H.; Bountra, C.; Fish, P. V.; Lee, K.; Schapira, M. Epigenetic protein families: a new frontier for drug discovery. *Nature Rev. Drug Discovery* **2012**, *11*, 384–400.

(17) Koh, S. S.; Chen, D.; Lee, Y.-H.; Stallcup, M. R. Synergistic Enhancement of Nuclear Receptor Function by p160 Coactivators and Two Coactivators with Protein Methyltransferase Activities. *J. Biol. Chem.* **2001**, *276*, 1089–1098.

(18) Wang, H.; Huang, Z.-Q.; Xia, L.; Feng, Q.; Erdjument-Bromage, H.; Strahl, B. D.; Briggs, S. D.; Allis, C. D.; Wong, J.; Tempst, P.; Zhang, Y. Methylation of Histone H4 at Arginine 3 Facilitating Transcriptional Activation by Nuclear Hormone Receptor. *Science* **2001**, *293*, 853–857.

(19) Anzick, S. L.; Kononen, J.; Walker, R. L.; Azorsa, D. O.; Tanner, M. M.; Guan, X.-Y.; Sauter, G.; Kallioniemi, O.-P.; Trent, J. M.; Meltzer, P. S. AIB1, a Steroid Receptor Coactivator Amplified in Breast and Ovarian Cancer. *Science* **1997**, *277*, 965–968.

(20) Torchia, J.; Rose, D. W.; Inostroza, J.; Kamei, Y.; Westin, S.; Glass, C. K.; Rosenfeld, M. G. The transcriptional co-activator p/CIP binds CBP and mediates nuclear-receptor function. *Nature* **1997**, *387*, 677–684.

(21) Lee, S.-K.; Anzick, S. L.; Choi, J.-E.; Bubendorf, L.; Guan, X.-Y.; Jung, Y.-K.; Kallioniemi, O. P.; Kononen, J.; Trent, J. M.; Azorsa, D.; Jhun, B.-H.; Cheong, J. H.; Lee, Y. C.; Meltzer, P. S.; Lee, J. W. A Nuclear Factor, ASC-2, as a Cancer-Amplified Transcriptional Coactivator Essential for Ligand-Dependent Transactivation by Nuclear Receptors in Vivo. *J. Biol. Chem.* **1999**, *274*, 34283–34293.

(22) Zhu, Y.; Qi, C.; Jain, S.; Le Beau, M. M.; Espinosa, R.; Atkins, G. B.; Lazar, M. A.; Yeldandi, A. V.; Rao, M. S.; Reddy, J. K. Amplification and overexpression of peroxisome proliferator-activated receptor binding protein (PBP/PPARBP) gene in breast cancer. *Proc. Natl. Acad. Sci. U. S. A.* **1999**, *96*, 10848–10853.

(23) Cheung, N.; Chan, L. C.; Thompson, A.; Cleary, M. L.; So, C. W. E. Protein arginine-methyltransferase-dependent oncogenesis. *Nature Cell Biol.* **2007**, *9*, 1208–1215.

(24) Scorilas, A.; Black, M. H.; Talieri, M.; Diamandis, E. P. Genomic Organization, Physical Mapping, and Expression Analysis of the Human Protein Arginine Methyltransferase 1 Gene. *Biochem. Biophys. Res. Commun.* **2000**, *278*, 349–359.

(25) Goulet, I.; Gauvin, G.; Boisvenue, S.; Cote, J. Alternative splicing yields protein arginine methyltransferase 1 isoforms with distinct activity, substrate specificity, and subcellular localization. *J. Biol. Chem.* **2007**, *282*, 33009–33021.

(26) Mathioudaki, K.; Papadokostopoulou, A.; Scorilas, A.; Xynopoulos, D.; Agnanti, N.; Talieri, M. The PRMT1 gene expression pattern in colon cancer. *Br. J. Cancer* **2008**, *99*, 2094–2099.

(27) Papadokostopoulou, A.; Mathioudaki, K.; Scorilas, A.; Xynopoulos, D.; Ardavanis, A.; Kouroumalis, E.; Talieri, M. Colon Cancer and Protein Arginine Methyltransferase 1 Gene Expression. *Anticancer Res.* **2009**, *29*, 1361−1366.
(28) Seligson, D. B.; Horvath, S.; Shi, T.; Yu, H.; Tze, S.; Grunstein, M.; Kurdistani, S. K. Global histone modification patterns predict risk of prostate cancer recurrence. *Nature* **2005**, *435*, 1262−1266.
(29) Cheng, D.; Côté, J.; Shaaban, S.; Bedford, M. T. The Arginine Methyltransferase CARM1 Regulates the Coupling of Transcription and mRNA Processing. *Mol. Cell* **2007**, *25*, 71−83.
(30) Li, H.; Park, S.; Kilburn, B.; Jelinek, M. A.; Henschen-Edman, A.; Aswad, D. W.; Stallcup, M. R.; Laird-Offringa, I. A. Lipopolysaccharide-Induced Methylation of HuR, an mRNA-Stabilizing Protein, by CARM1. *J. Biol. Chem.* **2002**, *277*, 44623−44630.
(31) Lee, J.; Bedford, M. T. PABP1 identified as an arginine methyltransferase substrate using high-density protein arrays. *EMBO Rep.* **2002**, *3*, 268−273.
(32) Fujiwara, T.; Mori, Y.; Chu, D. L.; Koyama, Y.; Miyata, S.; Tanaka, H.; Yachi, K.; Kubo, T.; Yoshikawa, H.; Tohyama, M. CARM1 Regulates Proliferation of PC12 Cells by Methylating HuD. *Mol. Cell. Biol.* **2006**, *26*, 2273−2285.
(33) Jeong, S. J.; Lu, H.; Cho, W. K.; Park, H. U.; Pise-Masison, C.; Brady, J. N. Coactivator-associated arginine methyltransferase 1 enhances transcriptional activity of the human T-cell lymphotropic virus type 1 long terminal repeat through direct interaction with Tax. *J. Virol.* **2006**, *80*, 10036−10044.
(34) Hong, H.; Kao, C.; Jeng, M.-H.; Eble, J. N.; Koch, M. O.; Gardner, T. A.; Zhang, S.; Li, L.; Pan, C.-X.; Hu, Z.; MacLennan, G. T.; Cheng, L. Aberrant expression of CARM1, a transcriptional coactivator of androgen receptor, in the development of prostate carcinoma and androgen-independent status. *Cancer* **2004**, *101*, 83−89.
(35) Majumder, S.; Liu, Y.; F., O. H., III; Mohler, J. L.; Whang, Y. E. Involvement of arginine methyltransferase CARM1 in androgen receptor function and prostate cancer cell viability. *Prostate* **2006**, *66*, 1292−1301.
(36) Feng, Q.; Yi, P.; Wong, J.; O'Malley, B. W. Signaling within a Coactivator Complex: Methylation of SRC-3/AIB1 Is a Molecular Switch for Complex Disassembly. *Mol. Cell. Biol.* **2006**, *26*, 7846−7857.
(37) Frietze, S.; Lupien, M.; Silver, P. A.; Brown, M. CARM1 regulates estrogen-stimulated breast cancer growth through up-regulation of E2F1. *Cancer Res.* **2008**, *68*, 301−306.
(38) Hassa, P. O.; Covic, M.; Bedford, M. T.; Hottiger, M. O. Protein Arginine Methyltransferase 1 Coactivates NF-κB-Dependent Gene Expression Synergistically with CARM1 and PARP1. *J. Mol. Biol.* **2008**, *377*, 668−678.
(39) An, W.; Kim, J.; Roeder, R. G. Ordered cooperative functions of PRMT1, p300, and CARM1 in transcriptional activation by p53. *Cell* **2004**, *117*, 735−748.
(40) Boger, R. H.; Sydow, K.; Borlak, J.; Thum, T.; Lenzen, H.; Schubert, B.; Tsikas, D.; Bode-Boger, S. M. LDL Cholesterol Upregulates Synthesis of Asymmetrical Dimethylarginine in Human Endothelial Cells: Involvement of *S*-Adenosylmethionine-Dependent Methyltransferases. *Circ. Res.* **2000**, *87*, 99−105.
(41) Tran, C. T. L.; Leiper, J. M.; Vallance, P. The DDAH/ADMA/NOS pathway. *Atherosclerosis Suppl.* **2003**, *4*, 33−40.
(42) Vallance, P.; Leiper, J. Cardiovascular Biology of the Asymmetric Dimethylarginine:Dimethylarginine Dimethylaminohydrolase Pathway. *Arterioscler., Thromb., Vasc. Biol.* **2004**, *24*, 1023−1030.
(43) Leiper, J.; Murray-Rust, J.; McDonald, N.; Vallance, P. *S*-Nitrosylation of dimethylarginine dimethylaminohydrolase regulates enzyme activity: Further interactions between nitric oxide synthase and dimethylarginine dimethylaminohydrolase. *Proc. Natl. Acad. Sci. U. S. A.* **2002**, *99*, 13527−13532.
(44) Leone, A.; Moncada, S.; Vallance, P.; Calver, A.; Collier, J. Accumulation of an endogenous inhibitor of nitric oxide synthesis in chronic renal failure. *Lancet* **1992**, *339*, 572−575.
(45) Leiper, J.; Nandi, M.; Torondel, B.; Murray-Rust, J.; Malaki, M.; O'Hara, B.; Rossiter, S.; Anthony, S.; Madhani, M.; Selwood, D.; Smith, C.; Wojciak-Stothard, B.; Rudiger, A.; Stidwill, R.; McDonald, N. Q.; Vallance, P. Disruption of methylarginine metabolism impairs vascular homeostasis. *Nature Med.* **2007**, *13*, 198−203.
(46) Chen, X.; Niroomand, F.; Liu, Z.; Zankl, A.; Katus, H. A.; Jahn, L.; Tiefenbacher, C. P. Expression of nitric oxide related enzymes in coronary heart disease. *Basic Res. Cardiol.* **2006**, *101*, 346−353.
(47) Maas, R. Pharmacotherapies and their influence on asymmetric dimethylargine (ADMA). *Vasc. Med.* **2005**, *10*, S49−S57.
(48) McKinsey, T. A.; Zhang, C. L.; Olson, E. N. Signaling chromatin to make muscle. *Curr. Opin. Cell Biol.* **2002**, *14*, 763−772.
(49) Yildirim, A. O.; Bulau, P.; Zakrzewicz, D.; Kitowska, K. E.; Weissmann, N.; Grimminger, F.; Morty, R. E.; Eickelberg, O. Increased Protein Arginine Methylation in Chronic Hypoxia: Role of Protein Arginine Methyltransferases. *Am. J. Respir. Cell Mol. Biol.* **2006**, *35*, 436−443.
(50) Hong, E.; Lim, Y.; Lee, E.; Oh, M.; Kwon, D. Tissue-specific and age-dependent expression of protein arginine methyltransferases (PRMTs) in male rat tissues. *Biogerontology* **2012**, *13*, 329−336.
(51) Ito, T.; Yadav, N.; Lee, J.; Furumatsu, T.; Yamashita, S.; Yoshida, K.; Taniguchi, N.; Hashimoto, M.; Tsuchiya, M.; Ozaki, T.; Lotz, M.; Bedford, M.; Asahara, H. Arginine methyltransferase CARM1/PRMT4 regulates endochondral ossification. *BMC Dev. Biol.* **2009**, *9*, 47.
(52) Batut, J.; Duboé, C.; Vandel, L. The Methyltransferases PRMT4/CARM1 and PRMT5 Control Differentially Myogenesis in Zebrafish. *PLoS One* **2011**, *6*, e25427.
(53) Wang, S.-C. M.; Dowhan, D. H.; Eriksson, N. A.; Muscat, G. E. O. CARM1/PRMT4 is necessary for the glycogen gene expression programme in skeletal muscle cells. *Biochem. J.* **2012**, *444*, 323−331.
(54) O'Brien, K. B.; Alberich-Jordà, M.; Yadav, N.; Kocher, O.; DiRuscio, A.; Ebralidze, A.; Levantini, E.; Sng, N. J. L.; Bhasin, M.; Caron, T.; Kim, D.; Steidl, U.; Huang, G.; Halmos, B.; Rodig, S. J.; Bedford, M. T.; Tenen, D. G.; Kobayashi, S. CARM1 is required for proper control of proliferation and differentiation of pulmonary epithelial cells. *Development* **2010**, *137*, 2147−2156.
(55) Tsankova, N.; Renthal, W.; Kumar, A.; Nestler, E. J. Epigenetic regulation in psychiatric disorders. *Nature Rev. Neurosci.* **2007**, *8*, 355−367.
(56) Wilson, C. B.; Rowell, E.; Sekimata, M. Epigenetic control of T-helper-cell differentiation. *Nature Rev. Immunol.* **2009**, *9*, 91−105.
(57) Copeland, R. A.; Solomon, M. E.; Richon, V. M. Protein methyltransferases as a target class for drug discovery. *Nature Rev. Drug Discovery* **2009**, *8*, 724−732.
(58) Cole, P. A. Chemical probes for histone-modifying enzymes. *Nature Chem. Biol.* **2008**, *4*, 590−597.
(59) Keppler, B. R.; Archer, T. K. Chromatin-modifying enzymes as therapeutic targets: Part 1. *Expert Opin. Ther. Targets* **2008**, *12*, 1301−1312.
(60) Spannhoff, A.; Sippl, W.; Jung, M. Cancer treatment of the future: Inhibitors of histone methyltransferases. *Int. J. Biochem. Cell Biol.* **2009**, *41*, 4−11.
(61) Strahl, B. D.; Briggs, S. D.; Brame, C. J.; Caldwell, J. A.; Koh, S. S.; Ma, H.; Cook, R. G.; Shabanowitz, J.; Hunt, D. F.; Stallcup, M. R.; Allis, C. D. Methylation of histone H4 at arginine 3 occurs in vivo and is mediated by the nuclear receptor coactivator PRMT1. *Curr. Biol.* **2001**, *11*, 996−1000.
(62) Migliori, V.; Phalke, S.; Bezzi, M.; Guccione, E. Arginine/lysine−methyl/methyl switches: biochemical role of histone arginine methylation in transcriptional regulation. *Epigenomics* **2010**, *2*, 119−137.
(63) Kim, D.; Lee, J.; Cheng, D.; Li, J.; Carter, C.; Richie, E.; Bedford, M. T. Enzymatic Activity Is Required for the in Vivo Functions of CARM1. *J. Biol. Chem.* **2010**, *285*, 1147−1152.
(64) Troffer-Charlier, N.; Cura, V.; Hassenboehler, P.; Moras, D.; Cavarelli, J. Functional insights from structures of coactivator-associated arginine methyltransferase 1 domains. *EMBO J.* **2007**, *26*, 4391−4401.

(65) Zhang, X.; Cheng, X. Structure of the predominant protein arginine methyltransferase PRMT1 and analysis of its binding to substrate peptides. *Structure* **2003**, *11*, 509−520.
(66) Zhang, X.; Zhou, L.; Cheng, X. Crystal structure of the conserved core of protein arginine methyltransferase PRMT3. *EMBO J.* **2000**, *19*, 3509−3519.
(67) Sack, J. S.; Thieffine, S.; Bandiera, T.; Fasolini, M.; Duke, G. J.; Jayaraman, L.; Kish, K. F.; Klei, H. E.; Purandare, A. V.; Rosettani, P.; Troiani, S.; Xie, D.; Bertrand, J. A. Structural basis for CARM1 inhibition by indole and pyrazole inhibitors. *Biochem. J.* **2011**, *436*, 331−339.
(68) Gui, S.; Wooderchak, W. L.; Daly, M. P.; Porter, P. J.; Johnson, S. J.; Hevel, J. M. Investigation of the Molecular Origins of Protein−Arginine Methyltransferase I (PRMT1) Product Specificity Reveals a Role for Two Conserved Methionine Residues. *J. Biol. Chem.* **2011**, *286*, 29118−29126.
(69) Yue, W. W.; Hassler, M.; Roe, S. M.; Thompson-Vale, V.; Pearl, L. H. Insights into histone code syntax from structural and biochemical studies of CARM1 methyltransferase. *EMBO J.* **2007**, *26*, 4402−4412.
(70) Obianyo, O.; Osborne, T. C.; Thompson, P. R. Kinetic Mechanism of Protein Arginine Methyltransferase 1. *Biochemistry* **2008**, *47*, 10420−10427.
(71) Rust, H. L.; Zurita-Lopez, C. I.; Clarke, S.; Thompson, P. R. Mechanistic Studies on Transcriptional Coactivator Protein Arginine Methyltransferase 1. *Biochemistry* **2011**, *50*, 3332−3345.
(72) Mai, A.; Altucci, L. Epi-drugs to fight cancer: from chemistry to cancer treatment, the road ahead. *Int. J. Biochem. Cell Biol.* **2009**, *41*, 199−213.
(73) Zheng, Y. G.; Wu, J.; Chen, Z.; Goodman, M. Chemical regulation of epigenetic modifications: opportunities for new cancer therapy. *Med. Res. Rev.* **2008**, *28*, 645−687.
(74) Amur, S. G.; Shanker, G.; Cochran, J. M.; Ved, H. S.; Pieringer, R. A. Correlation between inhibition of myelin basic protein (arginine) methyltransferase by sinefungoin and lack of compact myelin formation in cultures of cerebral cells from embryonic mice. *J. Neurosci. Res.* **1986**, *16*, 367−376.
(75) Cheng, D.; Yadav, N.; King, R. W.; Swanson, M. S.; Weinstein, E. J.; Bedford, M. T. Small molecule regulators of protein arginine methyltransferases. *J. Biol. Chem.* **2004**, *279*, 23892−23899.
(76) Mai, A.; Cheng, D.; Bedford, M. T.; Valente, S.; Nebbioso, A.; Perrone, A.; Brosch, G.; Sbardella, G.; De Bellis, F.; Miceli, M.; Altucci, L. Epigenetic Multiple Ligands: Mixed Histone/Protein Methyltransferase, Acetyltransferase, and Class III Deacetylase (Sirtuin) Inhibitors. *J. Med. Chem.* **2008**, *51*, 2279−2290.
(77) Mai, A.; Valente, S.; Cheng, D.; Perrone, A.; Ragno, R.; Simeoni, S.; Sbardella, G.; Brosch, G.; Nebbioso, A.; Conte, M.; Altucci, L.; Bedford, M. T. Synthesis and Biological Validation of Novel Synthetic Histone/Protein Methyltransferase Inhibitors. *ChemMedChem* **2007**, *2*, 987−991.
(78) Ragno, R.; Simeoni, S.; Castellano, S.; Vicidomini, C.; Mai, A.; Caroli, A.; Tramontano, A.; Bonaccini, C.; Trojer, P.; Bauer, I.; Brosch, G.; Sbardella, G. Small Molecule Inhibitors of Histone Arginine Methyltransferases: Homology Modeling, Molecular Docking, Binding Mode Analysis, and Biological Evaluations. *J. Med. Chem.* **2007**, *50*, 1241−1253.
(79) Spannhoff, A.; Heinke, R.; Bauer, I.; Trojer, P.; Metzger, E.; Gust, R.; Schule, R.; Brosch, G.; Sippl, W.; Jung, M. Target-Based Approach to Inhibitors of Histone Arginine Methyltransferases. *J. Med. Chem.* **2007**, *50*, 2319−2325.
(80) Spannhoff, A.; Machmur, R.; Heinke, R.; Trojer, P.; Bauer, I.; Brosch, G.; Schüle, R.; Hanefeld, W.; Sippl, W.; Jung, M. A novel arginine methyltransferase inhibitor with cellular activity. *Bioorg. Med. Chem. Lett.* **2007**, *17*, 4150−4153.
(81) Allan, M.; Manku, S.; Therrien, E.; Nguyen, N.; Styhler, S.; Robert, M.-F.; Goulet, A.-C.; Petschner, A. J.; Rahil, G.; Robert MacLeod, A.; Déziel, R.; Besterman, J. M.; Nguyen, H.; Wahhab, A. *N*-Benzyl-1-heteroaryl-3-(trifluoromethyl)-1*H*-pyrazole-5-carboxamides as inhibitors of co-activator associated arginine methyltransferase 1 (CARM1). *Bioorg. Med. Chem. Lett.* **2009**, *19*, 1218−1223.
(82) Huynh, T.; Chen, Z.; Pang, S.; Geng, J.; Bandiera, T.; Bindi, S.; Vianello, P.; Roletto, F.; Thieffine, S.; Galvani, A.; Vaccaro, W.; Poss, M. A.; Trainor, G. L.; Lorenzi, M. L.; Gottardis, M.; Jayaraman, L.; Purandare, A. V. Optimization of Pyrazole Inhibitors of Coactivator Associated Arginine Methyltransferase 1 (CARM1). *Bioorg. Med. Chem. Lett.* **2009**, *19*, 2924−2927.
(83) Purandare, A. V.; Chen, Z.; Huynh, T.; Pang, S.; Geng, J.; Vaccaro, W.; Poss, M. A.; Oconnell, J.; Nowak, K.; Jayaraman, L. Pyrazole inhibitors of coactivator associated arginine methyltransferase 1 (CARM1). *Bioorg. Med. Chem. Lett.* **2008**, *18*, 4438−4441.
(84) Therrien, E.; Larouche, G.; Manku, S.; Allan, M.; Nguyen, N.; Styhler, S.; Robert, M.-F.; Goulet, A.-C.; Besterman, J. M.; Nguyen, H.; Wahhab, A. 1,2-Diamines as inhibitors of co-activator associated arginine methyltransferase 1 (CARM1). *Bioorg. Med. Chem. Lett.* **2009**, *19*, 6725−6732.
(85) Bonham, K.; Hemmers, S.; Lim, Y.-H.; Hill, D. M.; Finn, M. G.; Mowen, K. A. Effects of a novel arginine methyltransferase inhibitor on T-helper cell cytokine production. *FEBS J.* **2010**, *277*, 2096−2108.
(86) Dowden, J.; Hong, W.; Parry, R. V.; Pike, R. A.; Ward, S. G. Toward the development of potent and selective bisubstrate inhibitors of protein arginine methyltransferases. *Bioorg. Med. Chem. Lett.* **2010**, *20*, 2103−2105.
(87) Feng, Y.; Li, M.; Wang, B.; Zheng, Y. G. Discovery and Mechanistic Study of a Class of Protein Arginine Methylation Inhibitors. *J. Med. Chem.* **2010**, *53*, 6028−6039.
(88) Obianyo, O.; Causey, C. P.; Osborne, T. C.; Jones, J. E.; Lee, Y.-H.; Stallcup, M. R.; Thompson, P. R. A Chloroacetamidine-Based Inactivator of Protein Arginine Methyltransferase 1: Design, Synthesis, and In Vitro and In Vivo Evaluation. *ChemBioChem* **2010**, *11*, 1219−1223.
(89) Osborne, T.; Weller Roska, R. L.; Rajski, S. R.; Thompson, P. R. In Situ Generation of a Bisubstrate Analogue for Protein Arginine Methyltransferase 1. *J. Am. Chem. Soc.* **2008**, *130*, 4574−4575.
(90) Selvi, B. R.; Batta, K.; Kishore, A. H.; Mantelingu, K.; Varier, R. A.; Balasubramanyam, K.; Pradhan, S. K.; Dasgupta, D.; Sriram, S.; Agrawal, S.; Kundu, T. K. Identification of a Novel Inhibitor of Coactivator-Associated Arginine Methyltransferase 1 (CARM1)-mediated Methylation of Histone H3 Arg-17. *J. Biol. Chem.* **2010**, *285*, 7143−7152.
(91) Wan, H.; Huynh, T.; Pang, S.; Geng, J.; Vaccaro, W.; Poss, M. A.; Trainor, G. L.; Lorenzi, M. V.; Gottardis, M.; Jayaraman, L.; Purandare, A. V. Benzo[*d*]imidazole Inhibitors of Coactivator Associated Arginine Methyltransferase 1 (CARM1)—Hit to Lead Studies. *Bioorg. Med. Chem. Lett.* **2009**, *19*, 5063−5066.
(92) Castellano, S.; Milite, C.; Ragno, R.; Simeoni, S.; Mai, A.; Limongelli, V.; Novellino, E.; Bauer, I.; Brosch, G.; Spannhoff, A.; Cheng, D.; Bedford, M. T.; Sbardella, G. Design, Synthesis and Biological Evaluation of Carboxy Analogues of Arginine Methyltransferase Inhibitor 1 (AMI-1). *ChemMedChem* **2010**, *5*, 398−414.
(93) Dillon, M. B. C.; Bachovchin, D. A.; Brown, S. J.; Finn, M. G.; Rosen, H.; Cravatt, B. F.; Mowen, K. A. Novel Inhibitors for PRMT1 Discovered by High-Throughput Screening Using Activity-Based Fluorescence Polarization. *ACS Chem. Biol.* **2012**, *7*, 1198−204.
(94) Obianyo, O.; Causey, C. P.; Jones, J. E.; Thompson, P. R. Activity-Based Protein Profiling of Protein Arginine Methyltransferase 1. *ACS Chem. Biol.* **2011**, *6*, 1127−1135.
(95) Hart, P. T.; Lakowski, T. M.; Thomas, D.; Frankel, A.; Martin, N. I. Peptidic Partial Bisubstrates as Inhibitors of the Protein Arginine *N*-Methyltransferases. *ChemBioChem* **2011**, *12*, 1427−1432.
(96) Dowden, J.; Pike, R. A.; Parry, R. V.; Hong, W.; Muhsen, U. A.; Ward, S. G. Small molecule inhibitors that discriminate between protein arginine *N*-methyltransferases PRMT1 and CARM1. *Org. Biomol. Chem.* **2011**, *9*, 7814−7821.
(97) Cheng, D.; Valente, S.; Castellano, S.; Sbardella, G.; Di Santo, R.; Costi, R.; Bedford, M. T.; Mai, A. Novel 3,5-Bis-(bromohydroxybenzylidene)piperidin-4-ones as Coactivator-Associated Arginine Methyltransferase 1 Inhibitors: Enzyme Selectivity and Cellular Activity. *J. Med. Chem.* **2011**, *54*, 4928−4932.

(98) Cheng, D.; Bedford, M. T. Xenoestrogens Regulate the Activity of Arginine Methyltransferases. *ChemBioChem* **2011**, *12*, 323−329.
(99) Bissinger, E.-M.; Heinke, R.; Spannhoff, A.; Eberlin, A.; Metzger, E.; Cura, V.; Hassenboehler, P.; Cavarelli, J.; Schüle, R.; Bedford, M. T.; Sippl, W.; Jung, M. Acyl derivatives of *p*-aminosulfonamides and dapsone as new inhibitors of the arginine methyltransferase hPRMT1. *Bioorg. Med. Chem.* **2011**, *19*, 3717−3731.
(100) Ragno, R.; Mai, A.; Simeoni, S.; Caroli, A.; Valente, S.; Perrone, A.; Castellano, S.; Sbardella, G. In *Small Molecule Inhibitors of Histone Arginine Methyltransferases: Updated Structure-Based 3-D QSAR Models with Improved Robustness and Predictive Ability*, Frontiers in CNS and Oncology Medicinal Chemistry, ACS-EFMC, Siena, Italy, October 7−9, 2007, COMC-010.
(101) Somei, M.; Yamada, F. Simple indole alkaloids and those with a non-rearranged monoterpenoid unit. *Nat. Prod. Rep.* **2005**, *22*, 73−103.
(102) Narayana, B.; Ashalatha, B. V.; Vijaya Raj, K. K.; Fernandes, J.; Sarojini, B. K. Synthesis of some new biologically active 1,3,4-oxadiazolyl nitroindoles and a modified Fischer indole synthesis of ethyl nitro indole-2-carboxylates. *Bioorg. Med. Chem.* **2005**, *13*, 4638−4644.
(103) Pierson, P. D.; Fettes, A.; Freichel, C.; Gatti-McArthur, S.; Hertel, C.; Huwyler, J. R.; Mohr, P.; Nakagawa, T.; Nettekoven, M.; Plancher, J.-M.; Raab, S.; Richter, H.; Roche, O.; Rodríguez Sarmiento, R. M. A.; Schmitt, M.; Schuler, F.; Takahashi, T.; Taylor, S.; Ullmer, C.; Wiegand, R. 5-Hydroxyindole-2-carboxylic Acid Amides: Novel Histamine-3 Receptor Inverse Agonists for the Treatment of Obesity. *J. Med. Chem.* **2009**, *52*, 3855−3868.
(104) Vicker, N.; Su, X.; Ganeshapillai, D.; Purohit, A.; Reed, M. J.; Potter, B. V. L. Preparation of arylsulfonylbenzazoles as inhibitors of 11-beta-hydroxy steroid dehydrogenase type 1 and type 2. Patent s2003-GB4590 2004037251, 20031023, 2003.
(105) Too, K.; Brown, D. M.; Holliger, P.; Loakes, D. Effect of a hydrogen bonding carboxamide group on universal bases. *Collect. Czech. Chem. Commun.* **2006**, *71*, 899−911.
(106) McBride, A. E.; Cook, J. T.; Stemmler, E. A.; Rutledge, K. L.; McGrath, K. A.; Rubens, J. A. Arginine Methylation of Yeast mRNA-Binding Protein Npl3 Directly Affects Its Function, Nuclear Export, and Intranuclear Protein Interactions. *J. Biol. Chem.* **2005**, *280*, 30888−30898.
(107) Gary, J. D.; Lin, W.-J.; Yang, M. C.; Herschman, H. R.; Clarke, S. The Predominant Protein−Arginine Methyltransferase from *Saccharomyces cerevisiae*. *J. Biol. Chem.* **1996**, *271*, 12585−12594.
(108) Henry, M. F.; Silver, P. A. A novel methyltransferase (Hmt1p) modifies poly(A)+-RNA-binding proteins. *Mol. Cell. Biol.* **1996**, *16*, 3668−3678.
(109) For these compounds, we were not able to obtain reproducible results due to solubility issues.
(110) Dal Piaz, F.; Tosco, A.; Eletto, D.; Piccinelli, A. L.; Moltedo, O.; Franceschelli, S.; Sbardella, G.; Remondelli, P.; Rastrelli, L.; Vesci, L.; Pisano, C.; De Tommasi, N. The Identification of a Novel Natural Activator of p300 Histone Acetyltranferase Provides New Insights into the Modulation Mechanism of this Enzyme. *ChemBioChem* **2010**, *11*, 818−827.
(111) Milite, C.; Castellano, S.; Benedetti, R.; Tosco, A.; Ciliberti, C.; Vicidomini, C.; Boully, L.; Franci, G.; Altucci, L.; Mai, A.; Sbardella, G. Modulation of the activity of histone acetyltransferases by long chain alkylidenemalonates (LoCAMs). *Bioorg. Med. Chem.* **2011**, *19*, 3690−3701.
(112) One RU represents the binding of 1 pg of protein per square mm.
(113) Coan, K. E. D.; Shoichet, B. K. Stoichiometry and Physical Chemistry of Promiscuous Aggregate-Based Inhibitors. *J. Am. Chem. Soc.* **2008**, *130*, 9606−9612.
(114) Giannetti, A. M.; Koch, B. D.; Browner, M. F. Surface Plasmon Resonance Based Assay for the Detection and Characterization of Promiscuous Inhibitors. *J. Med. Chem.* **2008**, *51*, 574−580.
(115) Lakowski, T. M.; Zurita-Lopez, C.; Clarke, S. G.; Frankel, A. Approaches to measuring the activities of protein arginine *N*-methyltransferases. *Anal. Biochem.* **2010**, *397*, 1−11.
(116) Lakowski, T. M.; Frankel, A. Sources of *S*-adenosyl-l-homocysteine background in measuring protein arginine *N*-methyltransferase activity using tandem mass spectrometry. *Anal. Biochem.* **2010**, *396*, 158−160.
(117) Yadav, N.; Lee, J.; Kim, J.; Shen, J.; Hu, M. C.; Aldaz, C. M.; Bedford, M. T. Specific protein methylation defects and gene expression perturbations in coactivator-associated arginine methyltransferase 1-deficient mice. *Proc. Natl. Acad. Sci. U. S. A.* **2003**, *100*, 6464−6468.
(118) Monod, J.; Wyman, J.; Changeux, J.-P. On the nature of allosteric transitions: a plausible model. *J. Mol. Biol.* **1965**, *12*, 88−118.
(119) Zorn, J. A.; Wells, J. A. Turning enzymes ON with small molecules. *Nature Chem. Biol.* **2010**, *6*, 179−188.
(120) A few PRMT1 activators, named AMAs, were previously reported by some of us. See: Cheng, D.; Yadav, N.; King, R. W.; Swanson, M. S.; Weinstein, E. J.; Bedford, M. T. Small molecule regulators of protein arginine methyltransferases. *J. Biol. Chem.* **2004**, *279*, 23892−23899 (reference 75)..
(121) Tachibana, M.; Sugimoto, K.; Fukushima, T.; Shinkai, Y. SET Domain-containing Protein, G9a, Is a Novel Lysine-preferring Mammalian Histone Methyltransferase with Hyperactivity and Specific Selectivity to Lysines 9 and 27 of Histone H3. *J. Biol. Chem.* **2001**, *276*, 25309−25317.
(122) Frankel, A.; Yadav, N.; Lee, J.; Branscombe, T. L.; Clarke, S.; Bedford, M. T. The Novel Human Protein Arginine *N*-Methyltransferase PRMT6 Is a Nuclear Enzyme Displaying Unique Substrate Specificity. *J. Biol. Chem.* **2002**, *277*, 3537−3543.
(123) Cooper, M. Label-free screening of biomolecular interactions. *Anal. Bioanal. Chem.* **2003**, *377*, 834−842.
(124) Johnsson, B.; Löfås, S.; Lindquist, G. Immobilization of proteins to a carboxymethyldextran-modified gold surface for biospecific interaction analysis in surface plasmon resonance sensors. *Anal. Biochem.* **1991**, *198*, 268−277.